Institut de Física d'Altes Energies

Optimized observable in non-leptonic decays

Based on JHEP 06 (2023) and arxiv: 2404.01186 [hep-ph]. In collaboration with Joaquim Matias, Sebastien Descotes-Genon and Gilberto Tetlalmatzi-Xolocotzi.

Status of the “famous” flavor anomalies

- Courtesy: J.M., “Beyond Flavor Anomalies IV”, Barcelona, 2023.

Non leptonics: Motivation and Introduction

- Expectation: tensions in rare $b \to s$ (maybe $b \to d$?) if tensions in semileptonics are due to NP.
- FCNC Non leptonic decays : loop suppressed in the SM : satisfactory amount of Experimental data.
- However, increased difficulty in controlling hadronic uncertainties w.r.t semileptonics.
- Theoretical approaches available:
  Phenomenological extraction using flavor symmetries (GTX, TH, *Eur.Phys.J.C* 82 (2022) 3, 210).
  Relate to other modes using symmetry (U-spin, SU(3)) (MG, DL, etal., Nucl.Phys. B675 (2003) 333-415 etc).
  Compute hadronic matrix elements (QCD Factorization) (MB, MN, etal, Phys. Lett. B 514 (2001) 315, etc).
- Work with penguin dominated modes with $B_{s,d}$ decaying to same final states: $K^{(*)}\,\overline{K}^{(*)}, K^*\phi$.
- Use them to construct observables (ratios of (longitudinal for vector-vector) branching ratios). with reduced sensitivities to hadronic uncertainties (endpoint divergences).
- Use these observables to look for effects that might potentially be beyond SM: New Physics.

Amplitude and "Δ"

- $\bar{A}_f = A(\bar{B}_q \to F_1 F_2) = \lambda_u^{(q)} T_q + \lambda_c^{(q)} P_q = \lambda_u^{(q)} \Delta_q - \lambda_t^{(q)} P_q$ (unitarity).
- Δ_q is free of endpoint divergences (PRL 97 (2006) 061801: SDG, JM, JV). Because:

$$T_q = A^q_{K^*K^*}\left(\alpha_4^u - \frac{1}{2}\alpha_{4,EW}^u + \beta_3^u + 2\beta_4^u - \frac{1}{2}\beta_{3,EW}^u - \beta_{4,EW}^u\right)$$
$$P_q = A^q_{K^*K^*}\left(\alpha_4^c - \frac{1}{2}\alpha_{4,EW}^c + \beta_3^c + 2\beta_4^c - \frac{1}{2}\beta_{3,EW}^c - \beta_{4,EW}^c\right)$$

- Where,

Vertex — Hard spectator — Penguin

$$\alpha_i^p(M_1 M_2) \propto \left[V_i(M_2) + \frac{4\pi^2}{N_c} H_i(M_1 M_2)\right] + P_i^p(M_2)$$

H_i → $\propto X_H^{M_1} \sim \ln\left(\frac{m_b}{\Lambda_{QCD}}\right)$

(soft gluon spectator int, divergent, power suppressed, universal)

- β_i^p: Penguin annihilation, $\beta_{i,EW}^p$: Electroweak penguin annihilation

$\propto X_A^{M_1}$ ~ Endpoint divergence $\sim \ln\left(\frac{m_b}{\Lambda_{QCD}}\right)$ (universal) **Enter the same way in T and P (at LO in QCD).**

These divergences are responsible for the model dependence of the analysis.

The “L” observable: definition and features

- $$L = \kappa \left|\frac{P_s}{P_d}\right|^2 \left[\frac{1+|\alpha^s|^2\left|\frac{\Delta_s}{P_s}\right|^2+2Re\left(\frac{\Delta_s}{P_s}\right)Re(\alpha_s)}{1+|\alpha^d|^2\left|\frac{\Delta_d}{P_d}\right|^2+2Re\left(\frac{\Delta_d}{P_d}\right)Re(\alpha_d)}\right]$$

CKM

Dominant contribution

~ 1

- Relative uncertainty less than relative uncertainties in branching ratios.
- Generally asymmetric SM distribution since ratio. Degree of asymmetry depends on the relative uncertainty on the denominator.
- Dominant contribution to the uncertainties from form factors and not annihilation which are dominant sources for branching ratio uncertainties (use of u-spin symmetry).
- Renders value of ratio ‘L’ robust: independent of dynamical model/symmetry considerations used to calculate its value.

Diagrams: $K^{(*)}\overline{K}^{(*)}$

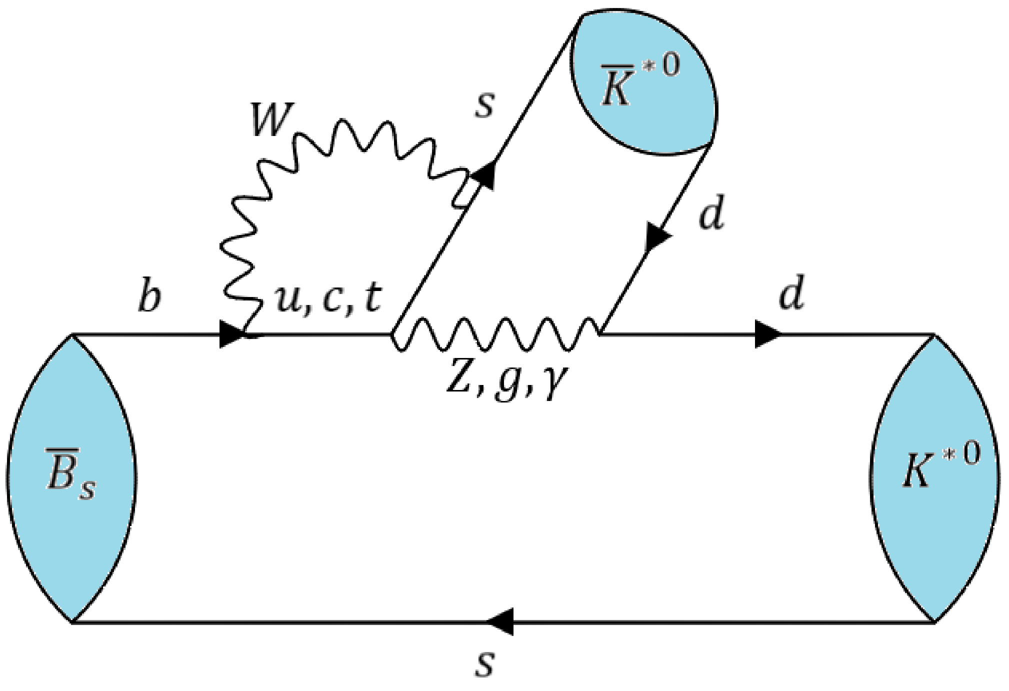

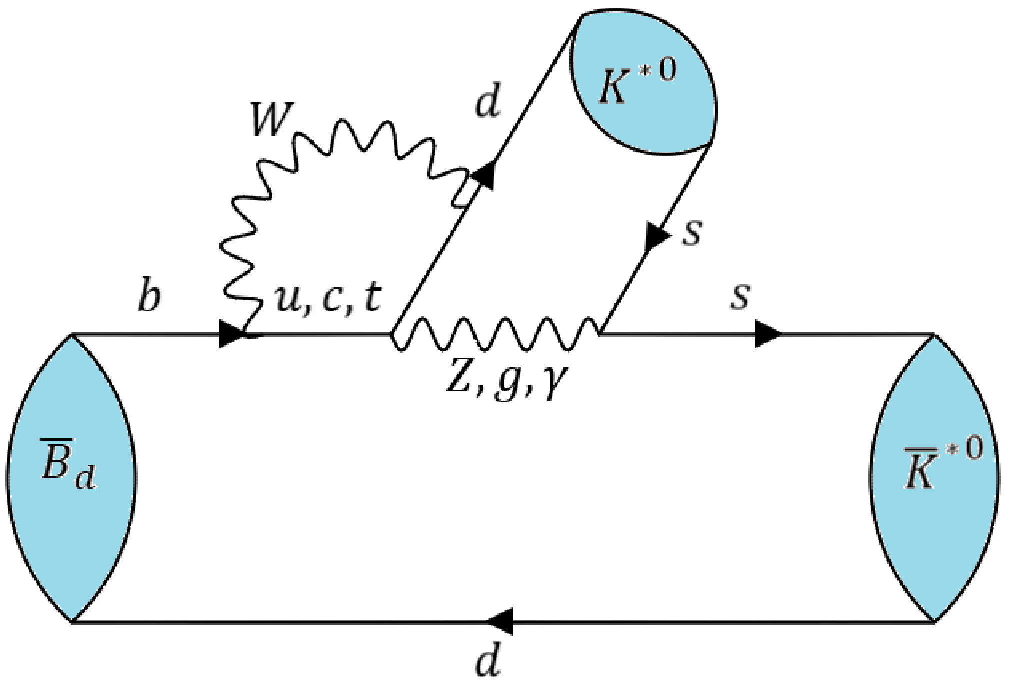

Diagrams: $K^*\phi$

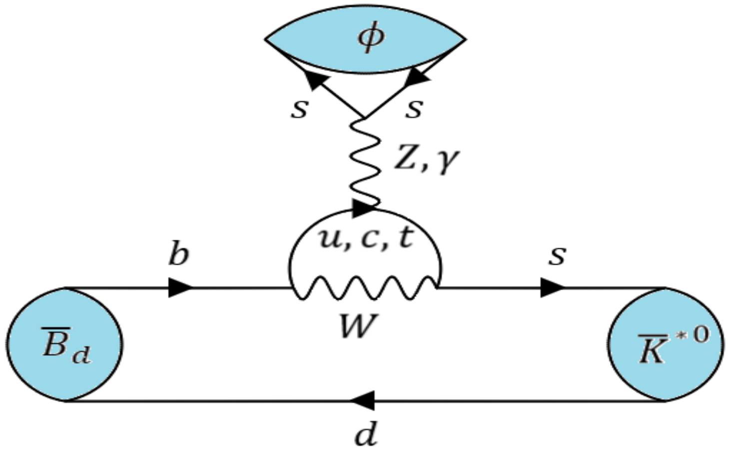

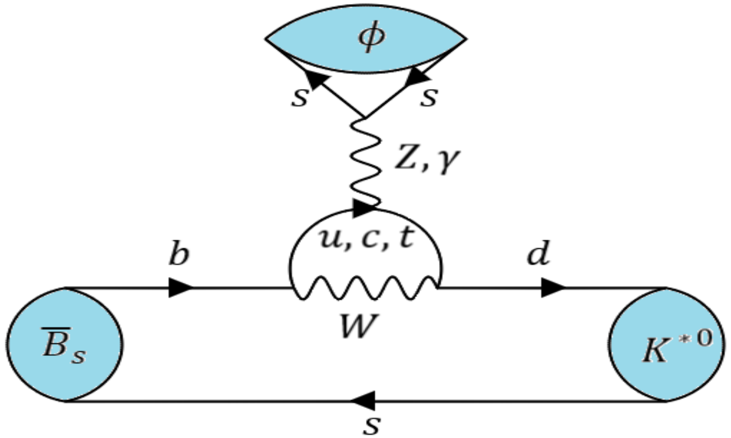

Same as
$K^{(*)}K^{(*)}$

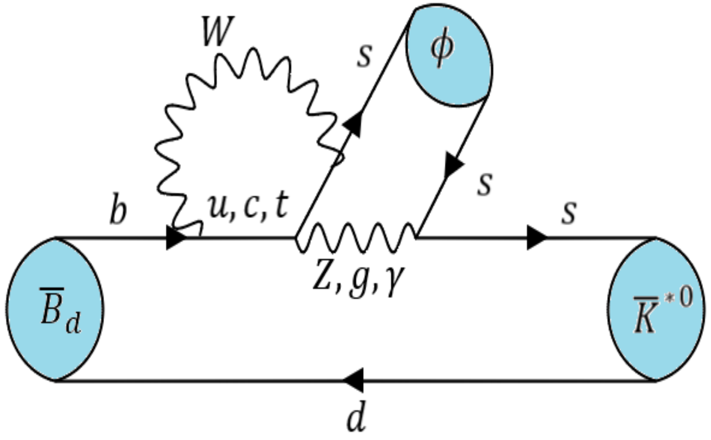

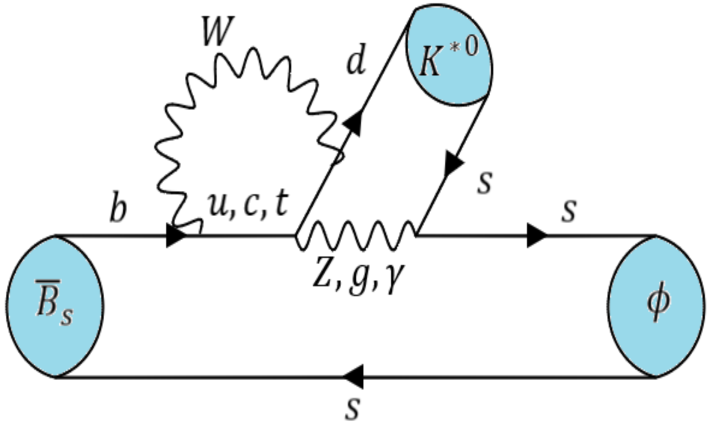

Theory vs experiment: Current status

Observable	SM (QCDF)	Experiment	Deviation
$10^6 BR(\bar{B}_d \to K^0\ \bar{K}^0)$	$1.09^{+0.29}_{-0.20}$	1.21 ± 0.16	0.4σ
$10^7 BR(\bar{B}_d \to K^{*0}\ \bar{K}^{*0})_L$	$2.27^{+0.99}_{-0.74}$	$6.04^{+1.81}_{-1.78}$	1.8σ
$10^5 BR(\bar{B}_s \to K^0\ \bar{K}^0)$	$2.80^{+0.89}_{-0.62}$	1.76 ± 0.33	1.6σ
$10^6 BR(\bar{B}_s \to K^{*0}\ \bar{K}^{*0})_L$	$4.36^{+2.23}_{-1.65}$	$2.62^{+0.85}_{-0.75}$	0.9σ
$10^6 BR(\bar{B}_d \to\ \bar{K}^{*0}\phi)_L$	$4.53^{+2.16}_{-1.80}$	$4.96^{+0.31}_{-0.30}$	0.3σ
$10^7 BR(\bar{B}_s \to K^{*0}\ \phi)_L$	$2.19^{+1.05}_{-0.94}$	$5.56^{+2.78}_{-2.27}$	1.3σ
$\mathrm{L}_{K^*\bar{K}^*}$	$19.53^{+9.14}_{-6.64}$	4.43 ± 0.92	2.6σ
$\mathrm{L}_{K\bar{K}}$	$26.00^{+3.88}_{-3.59}$	14.58 ± 3.37	2.4σ
$\mathrm{L}_{K^*\phi}$	$22.04^{+7.06}_{-4.88}$	$8.80^{+6.07}_{-2.97}$	1.5σ

Operator basis and SM Wilson Coefficients

$$H_{\text{eff}} = \frac{G_F}{\sqrt{2}} \sum_{p=c,u} \lambda_p^{(s,d)} \Big(\mathcal{C}^p_{1s,d} Q^p_{1s,d} + \mathcal{C}^p_{2s,d} Q^p_{2s,d} + \sum_{i=3...10} \mathcal{C}_{is,d} Q_{is,d} + \mathcal{C}_{7\gamma s,d} Q_{7\gamma s,d} + \mathcal{C}_{8gs,d} Q_{8gs,d} \Big)$$

$$Q_{4f} = (\bar{f}_i b_j)_{V-A} \sum_q (\bar{q}_j q_i)_{V-A}$$

$$Q_{8gf} = \frac{-g_s}{8\pi^2} m_b \, \bar{f} \sigma_{\mu\nu} (1+\gamma_5) G^{\mu\nu} b$$

$$Q_{6f} = (\bar{f}_i b_j)_{V-A} \sum_q^{q} (\bar{q}_j q_i)_{V+A}$$

SM Wilson Coefficients (at $\mu = 4.18$ GeV)					
$\mathcal{C}_1$	$\mathcal{C}_2$	$\mathcal{C}_3$	$\mathcal{C}_4$	$\mathcal{C}_5$	$\mathcal{C}_6$
1.082	-0.191	0.014	-0.036	0.009	-0.042
$\mathcal{C}_7/\alpha_{em}$	$\mathcal{C}_8/\alpha_{em}$	$\mathcal{C}_9/\alpha_{em}$	$\mathcal{C}_{10}/\alpha_{em}$	$\mathcal{C}_{7\gamma}^{\text{eff}}$	$\mathcal{C}_{8g}^{\text{eff}}$
-0.011	0.060	-1.254	0.224	-0.318	-0.151

$C_{4d,s}^{NP}\ (\bar{B}_{d,s} \rightarrow K^{(*)}\bar{K}^{(*)})$

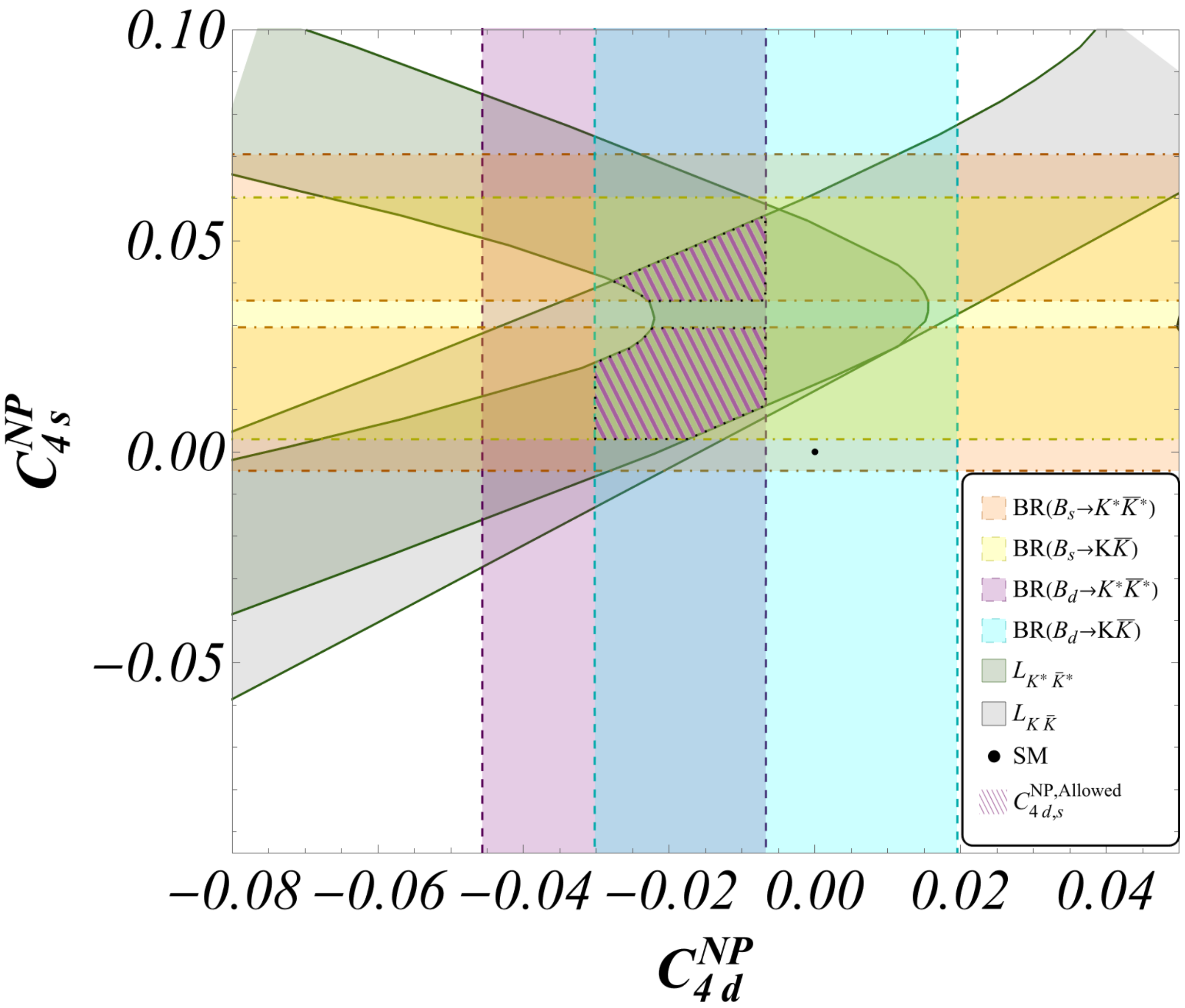

$$Q_{4f} = (\bar{f}_i b_j)_{V-A} \sum_q (\bar{q}_j q_i)_{V-A}$$

$C^{NP}_{4d,s}\ (\bar{B}_{s,(d)} \to \mathrm{K}^*(\bar{K}^*)\phi)$

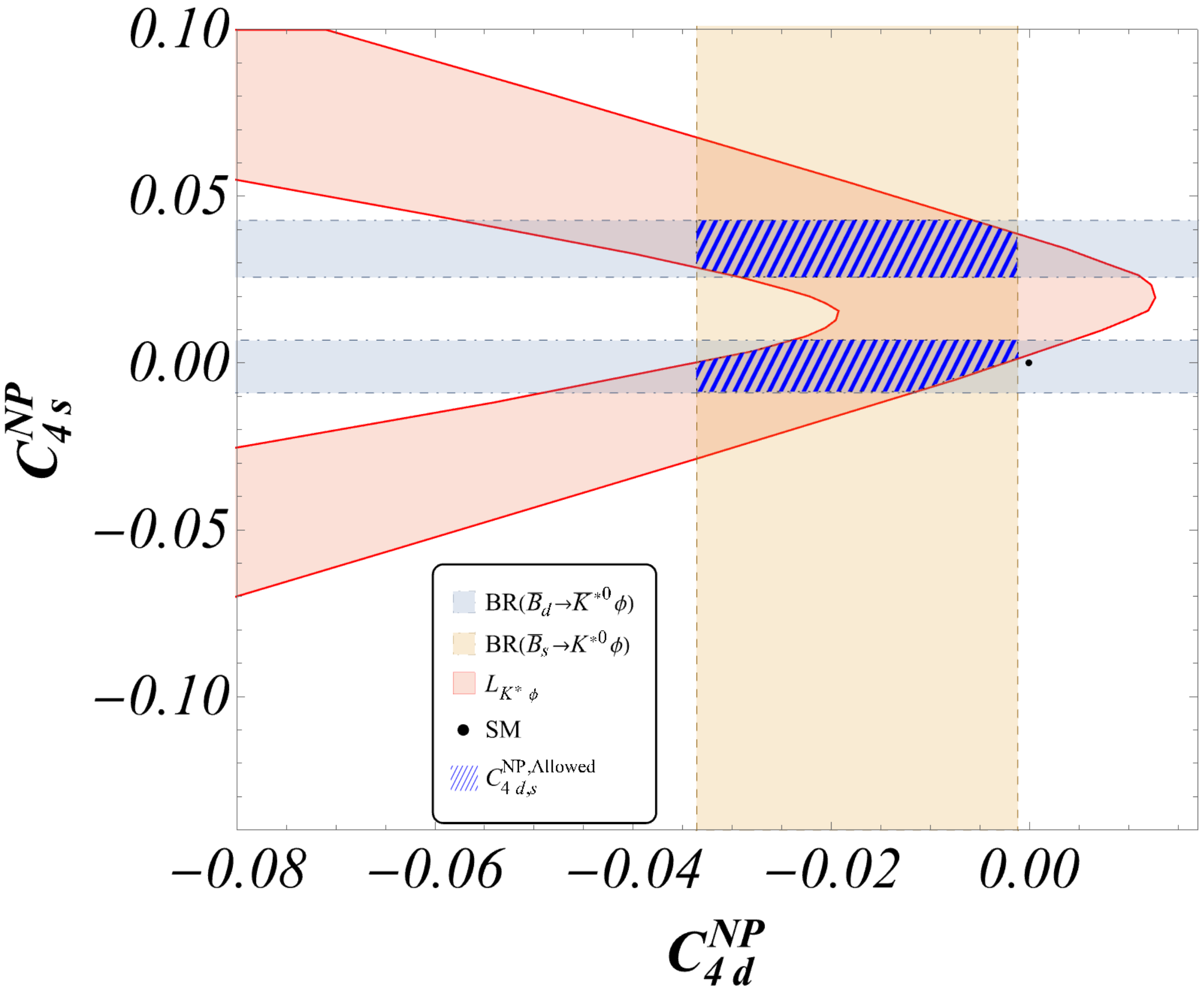

$C_{4d,s}^{NP}$ ($\mathrm{K}^{(*)}\overline{K}^{(*)}$, $\mathrm{K}^{*}\phi$ *combined*)

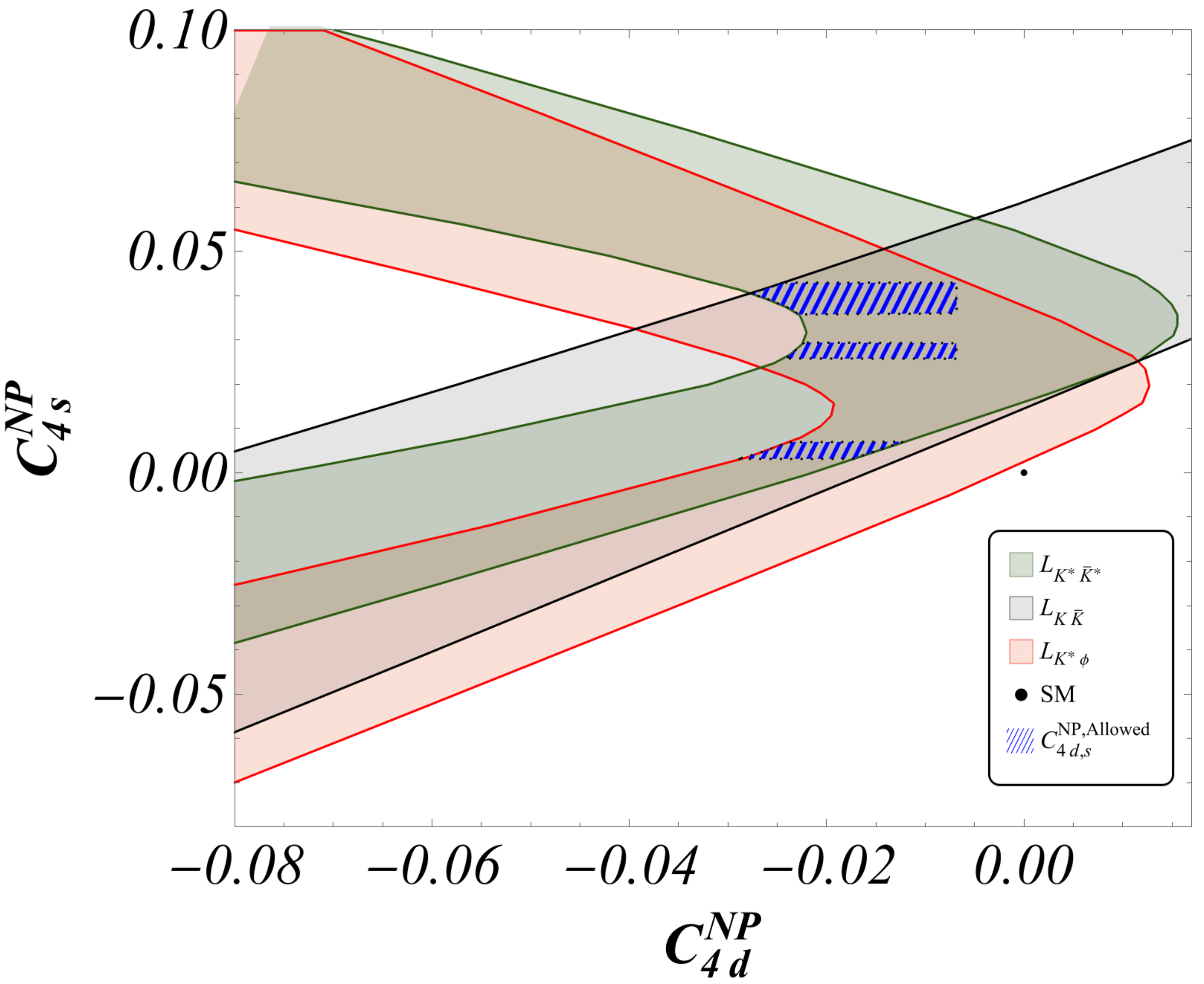

$C^{NP}_{8gd,s}\ (\bar{B}_{d,s} \to K^{(*)}\bar{K}^{(*)})$

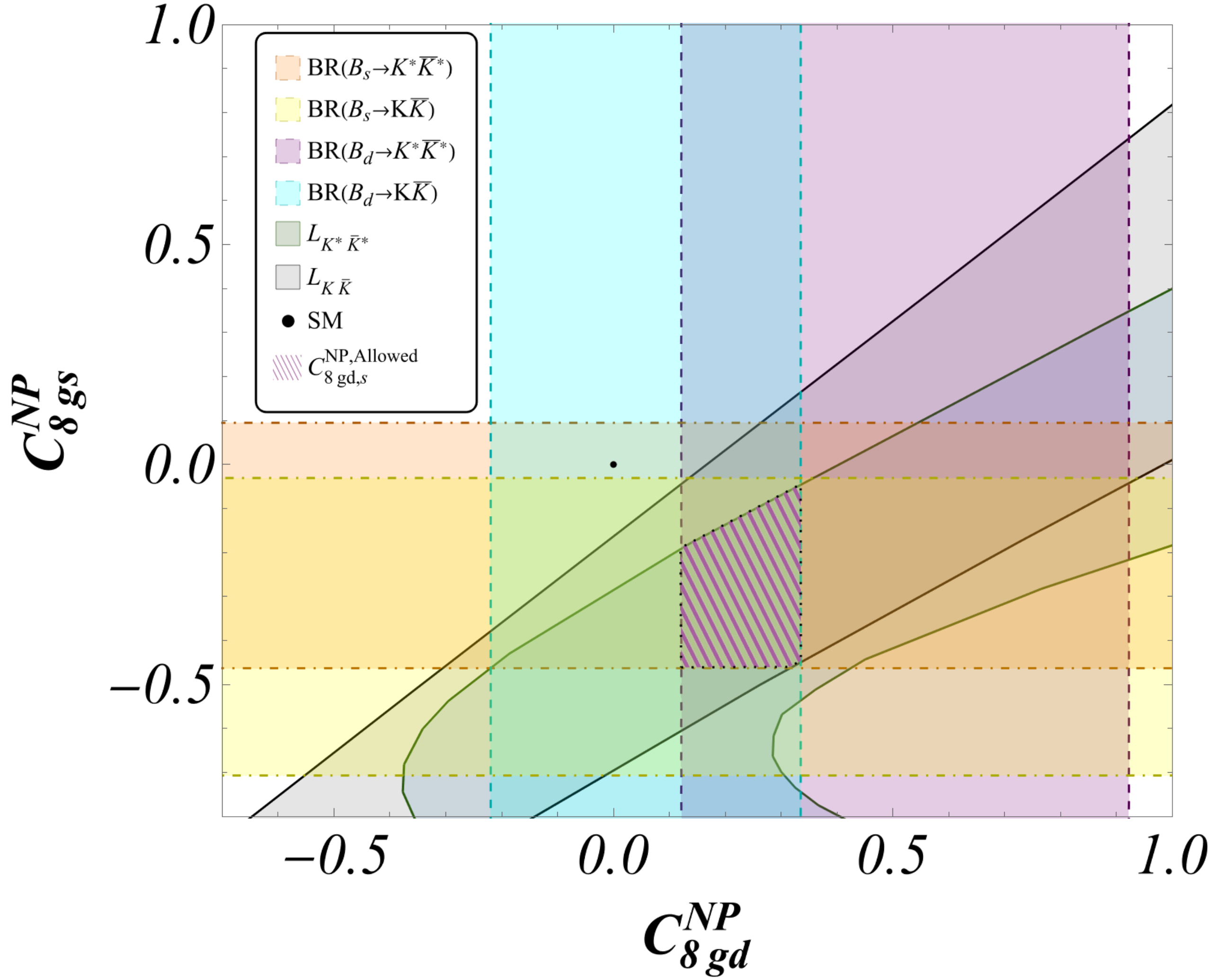

$$Q_{8gf} = \frac{-g_s}{8\pi^2}\, m_b\, \bar{f}\sigma_{\mu\nu}(1+\gamma_5)G^{\mu\nu} b$$

$C_{8gd,s}^{NP}(\bar{B}_{s,(d)} \to K^*(\bar{K}^*)\phi)$

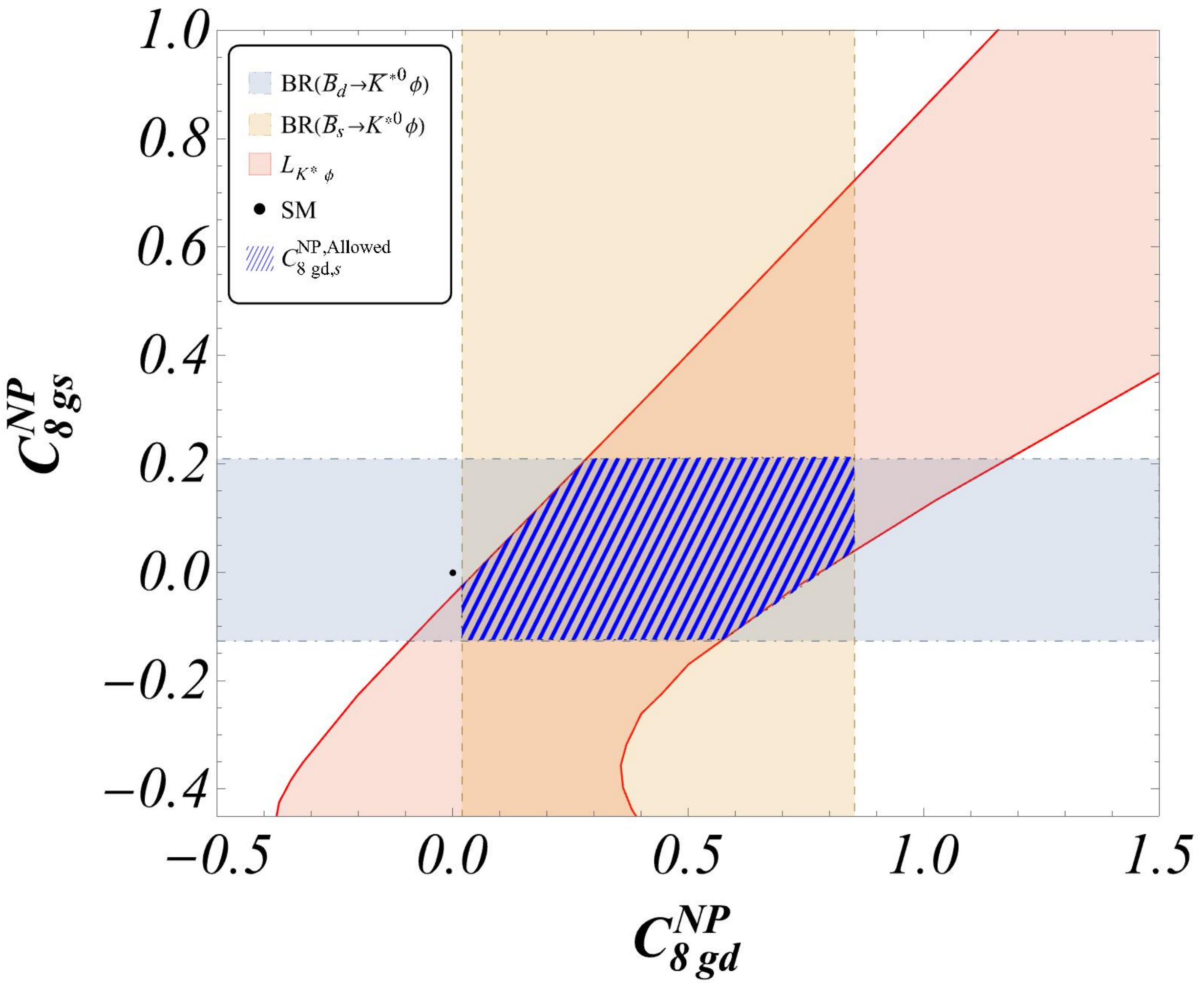

$C^{NP}_{8gd,s}(\mathrm{K}^{(*)}\bar{K}^{(*)}, \mathrm{K}^{*}\phi\ combined)$

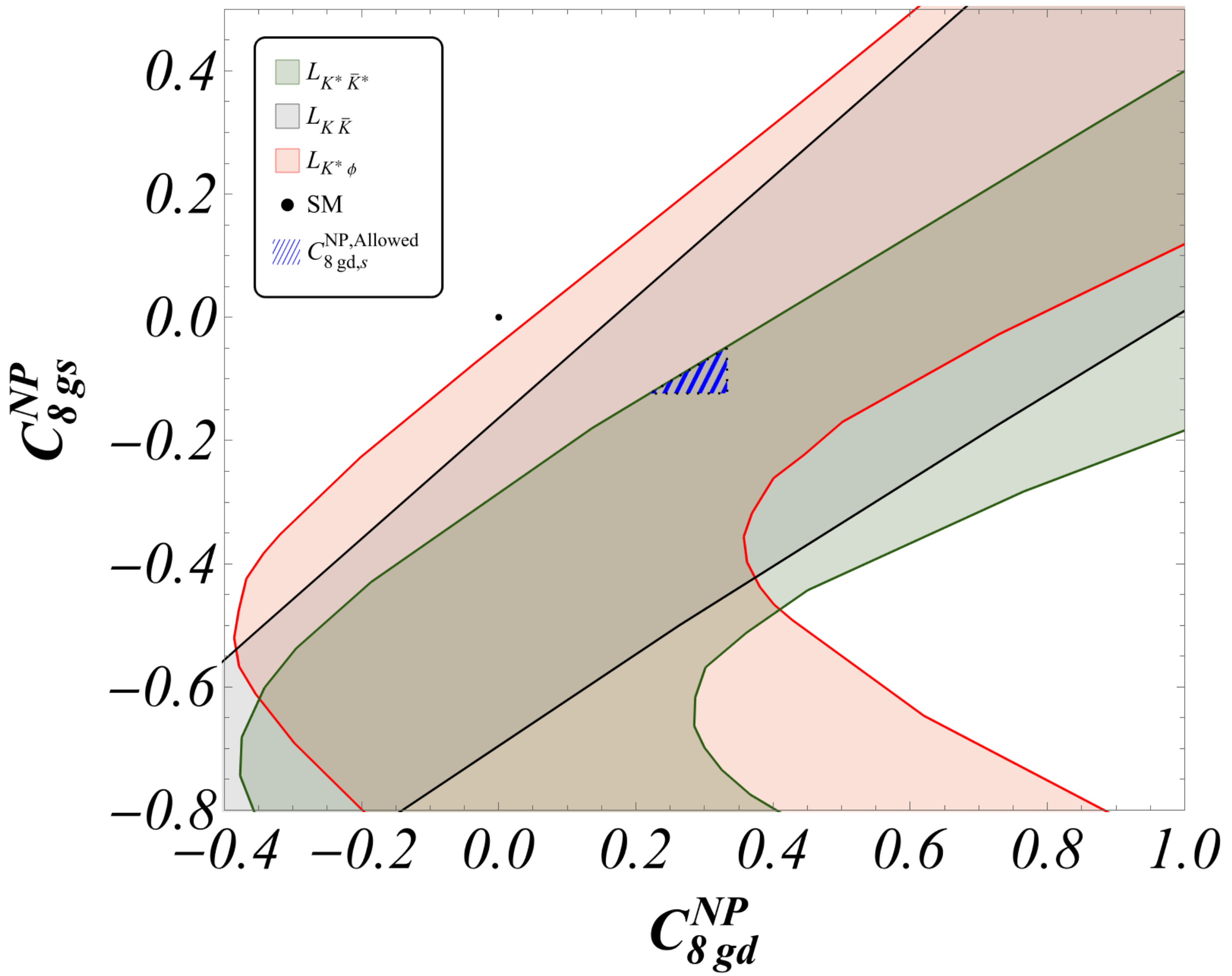

Theory vs experiment: Pseudoscalar Vector modes

Observable	SM (QCDF)	Experiment	Deviation
$10^5(BR(\bar{B}_s \to K^{*0}\,\bar{K}^0) + \text{c.c.})$	$0.83^{+0.50}_{-0.25}$	$1.98 \pm 0.28 \pm 0.50$	1.4σ
$10^6 BR(\bar{B}_d \to \bar{K}^0 \phi)$	$4.28^{+2.71}_{-1.50}$	7.3 ± 0.7	1.3σ

Effect of BR($\overline{B}_s \to K^* \overline{K} + c.c.$) and BR($\overline{B}_d \to \overline{K}\phi$) on $C^{NP}_{4d,s}$ plane

BR($\overline{B}_s \to K^* \overline{K} + c.c.$)

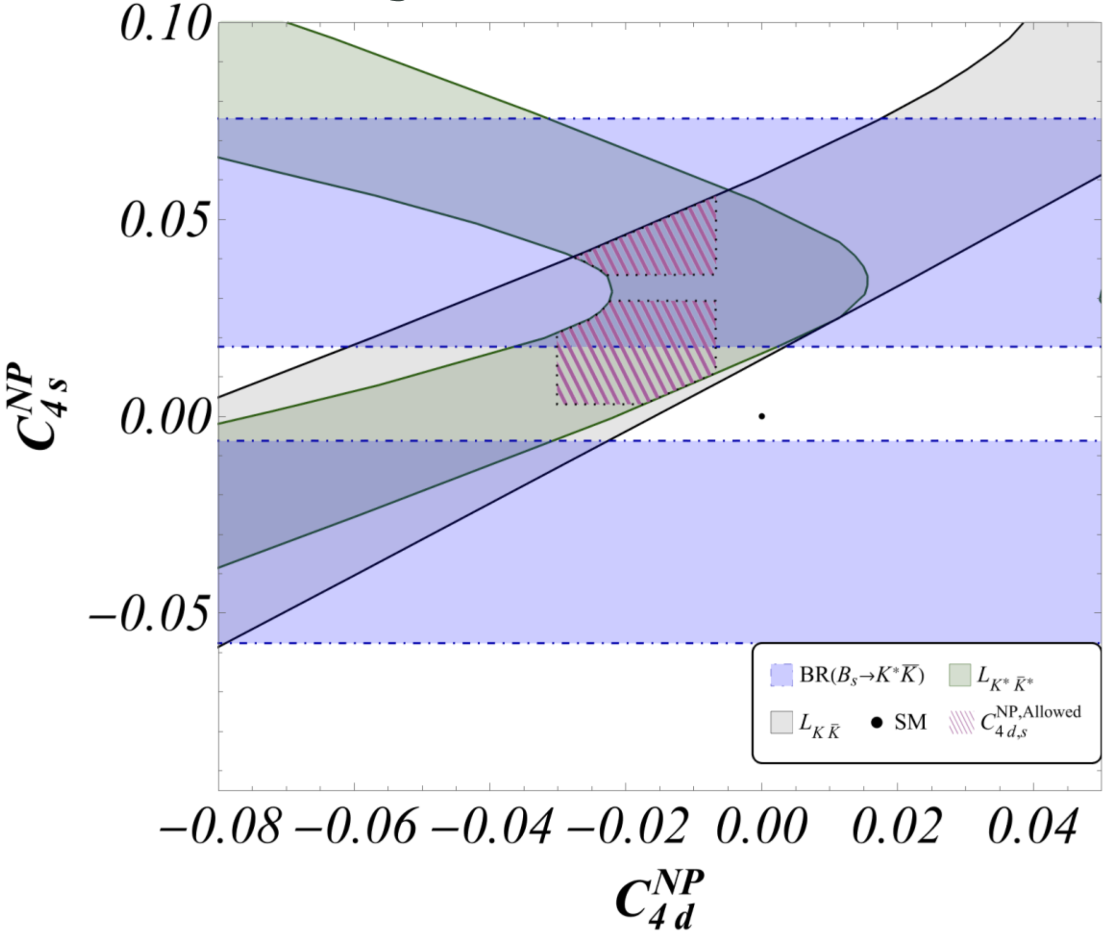

BR($\overline{B}_d \to \overline{K}\phi$)

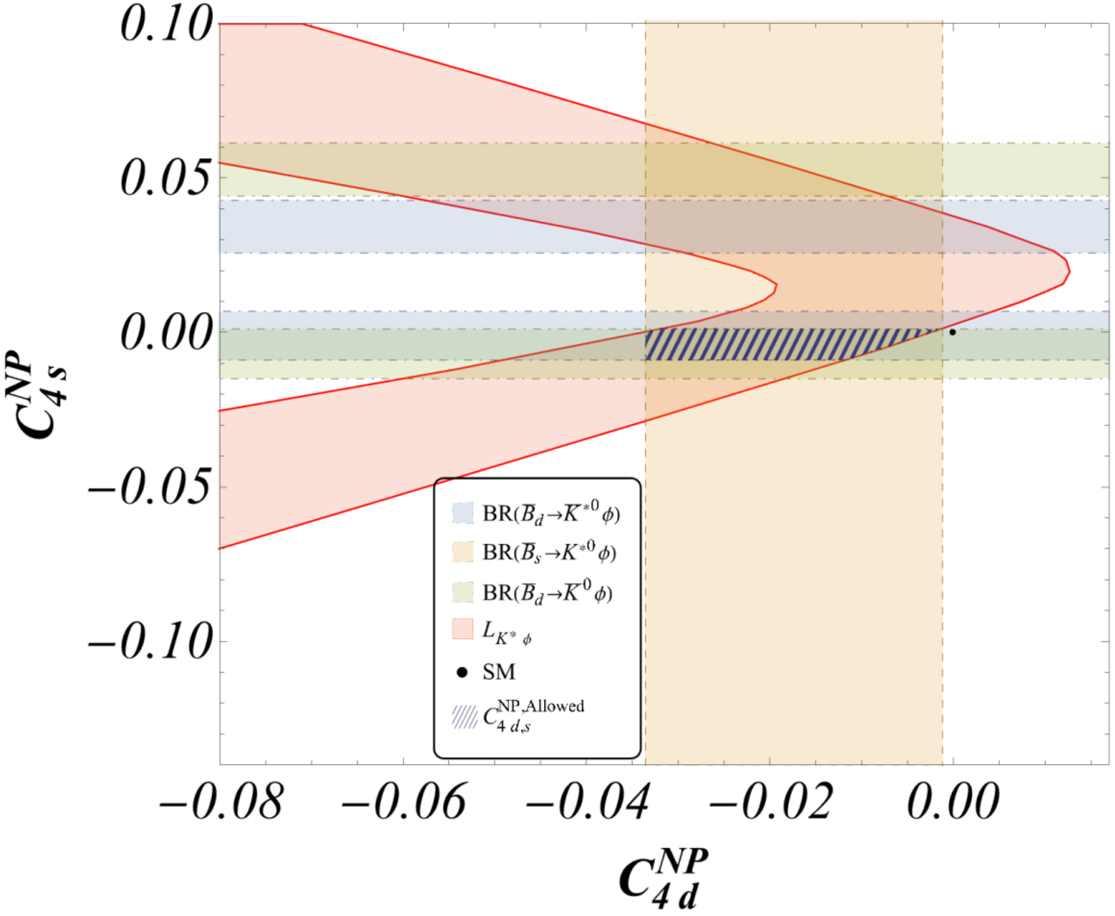

Effect of BR($\bar{B}_s \to K^*\bar{K} + c.c.$) and BR ($\bar{B}_d \to \bar{K}\phi$) on $C_{4d,s}^{NP}$ plane

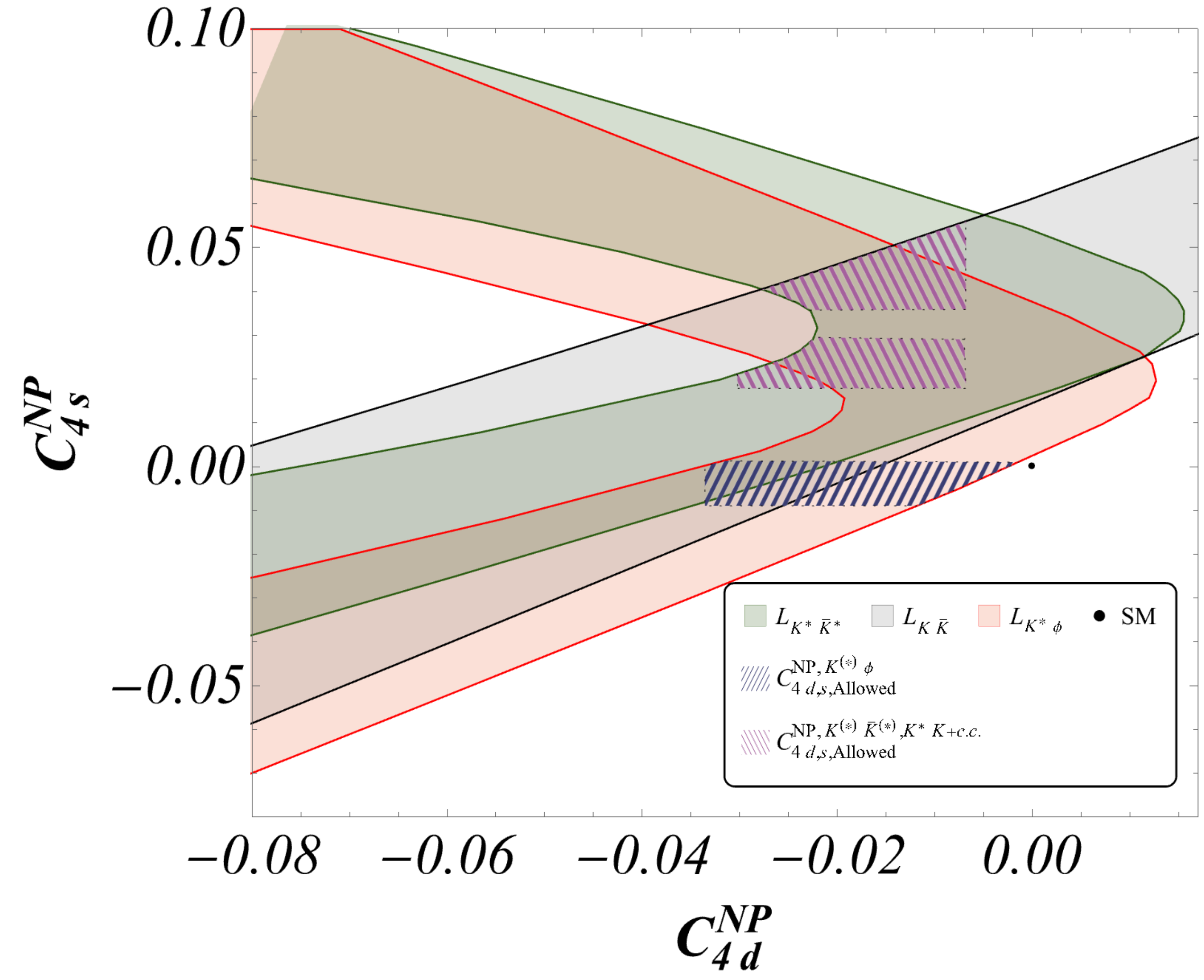

Effect of the mixed modes ($\bar{B}_s \to K^* \bar{K} + c.c.$) and ($\bar{B}_d \to \bar{K}\phi$) on $C^{NP}_{8gd,s}$ plane

BR($\bar{B}_s \to K^* \bar{K} + c.c.$)

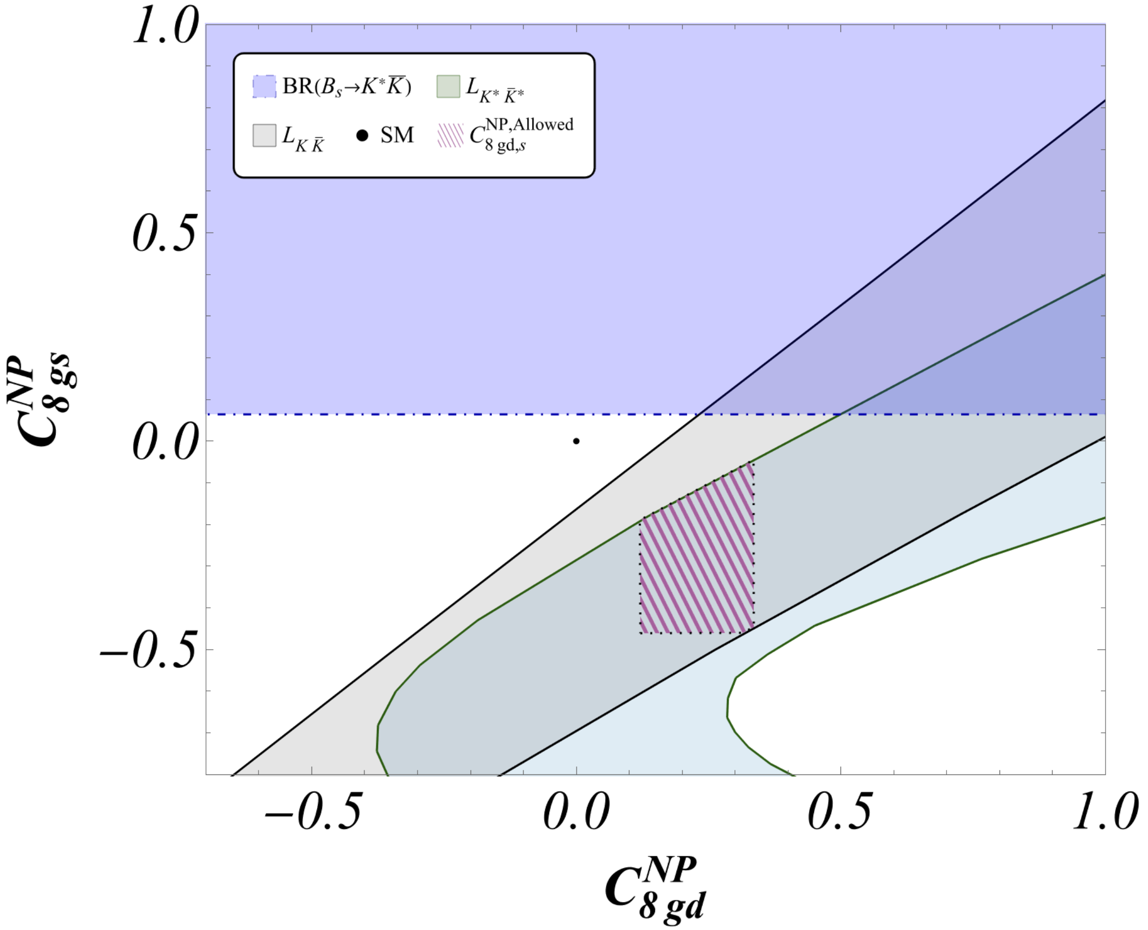

BR($\bar{B}_d \to \bar{K}\phi$)

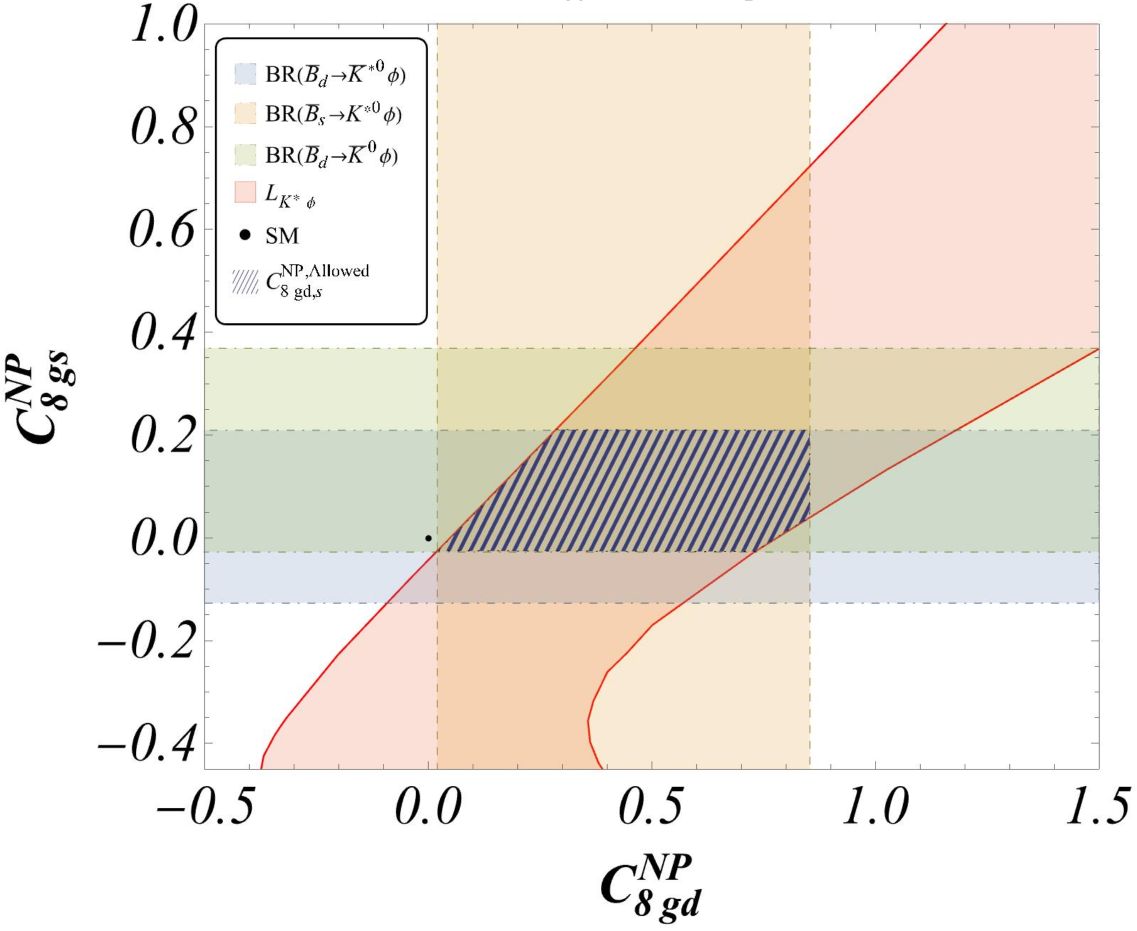

Effect of BR($\bar{B}_d \to \bar{K}\phi$) on $C_{8gd,s}^{NP}$ plane

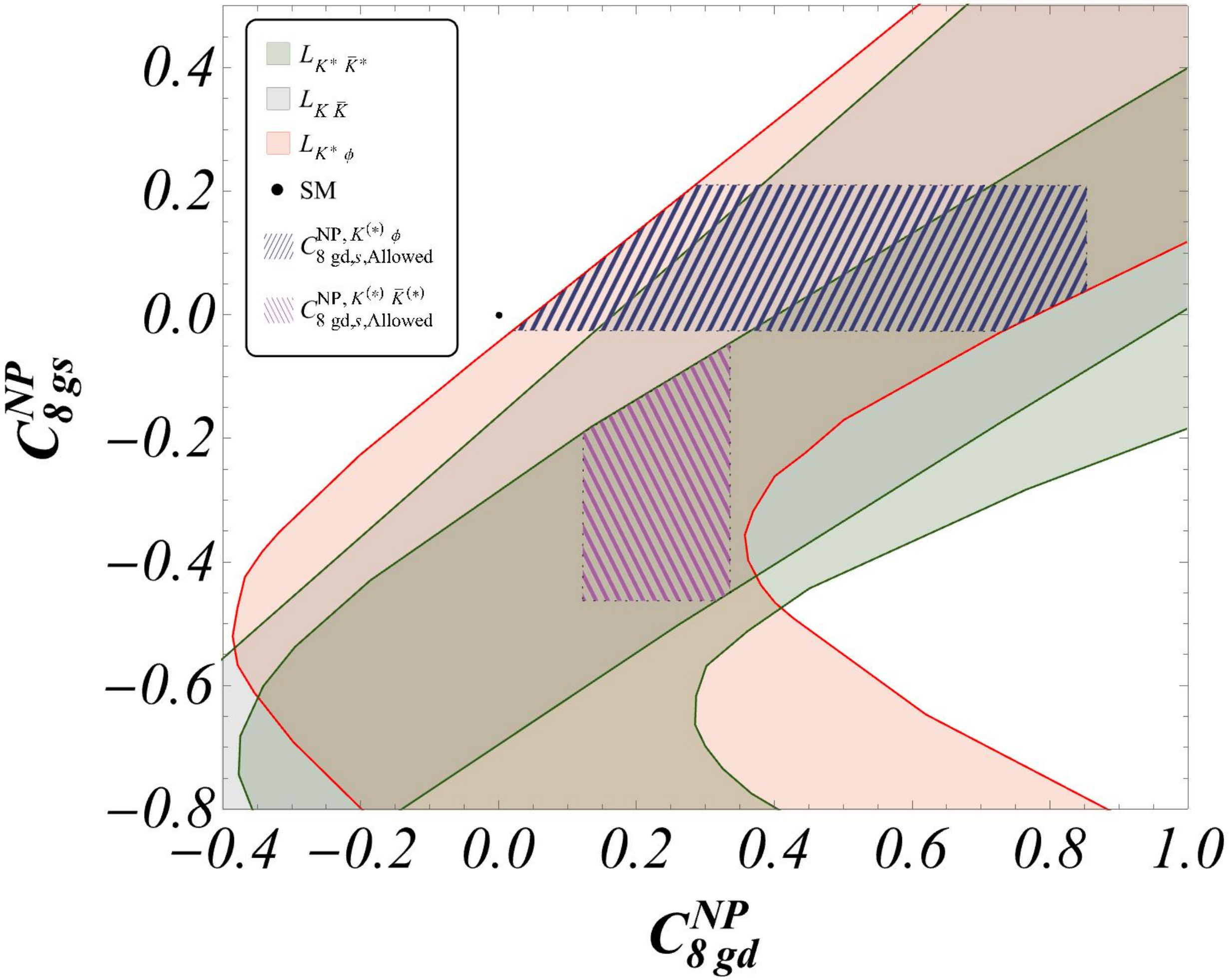

- $K^{(*)}K^{(*)}$ modes already incompatible with constraints from K^*K modes assuming NP affects $O_{8g,s,d}$ (previous slide).
- We find $K^{(*)}K^{(*)}$ also incompatible with $K^{(*)}\phi$ modes assuming NP affects $O_{8g,s,d}$.

Recap: Lessons from one operator scenarios

- Assuming NP affects either $Q_{4d,s}$ or $Q_{8gd,s}$ we find common overlaps for PP and VV modes.
- Result of including $K^*\phi$ modes with $K^{(*)}K^{(*)}$modes: "allowed" range of NP values is greater for $b \to d$ as compared to $b \to s$.
  - **……..pattern broken when pseudoscalar vector modes included.**
- NP affects $Q_{4d,s}$: mutual overlap among $K^{(*)}\phi$. Also among $K^{(*)}K^{(*)}, K^*K$. But not together.
- NP affects $Q_{4d,s}$: mutual overlap among $K^{(*)}\phi$. No mutual overlap among $K^{(*)}K^{(*)}, K^*K$.
- No common one operator explanation is possible. **Two operators (involving Q_6)?!**
- **Appeal to LHCb: Measurement of BR($\overline{B}_d \to \overline{K}\phi$) required to confirm or dismiss this picture.**

Two operator scenarios: $Q_4 - Q_6$

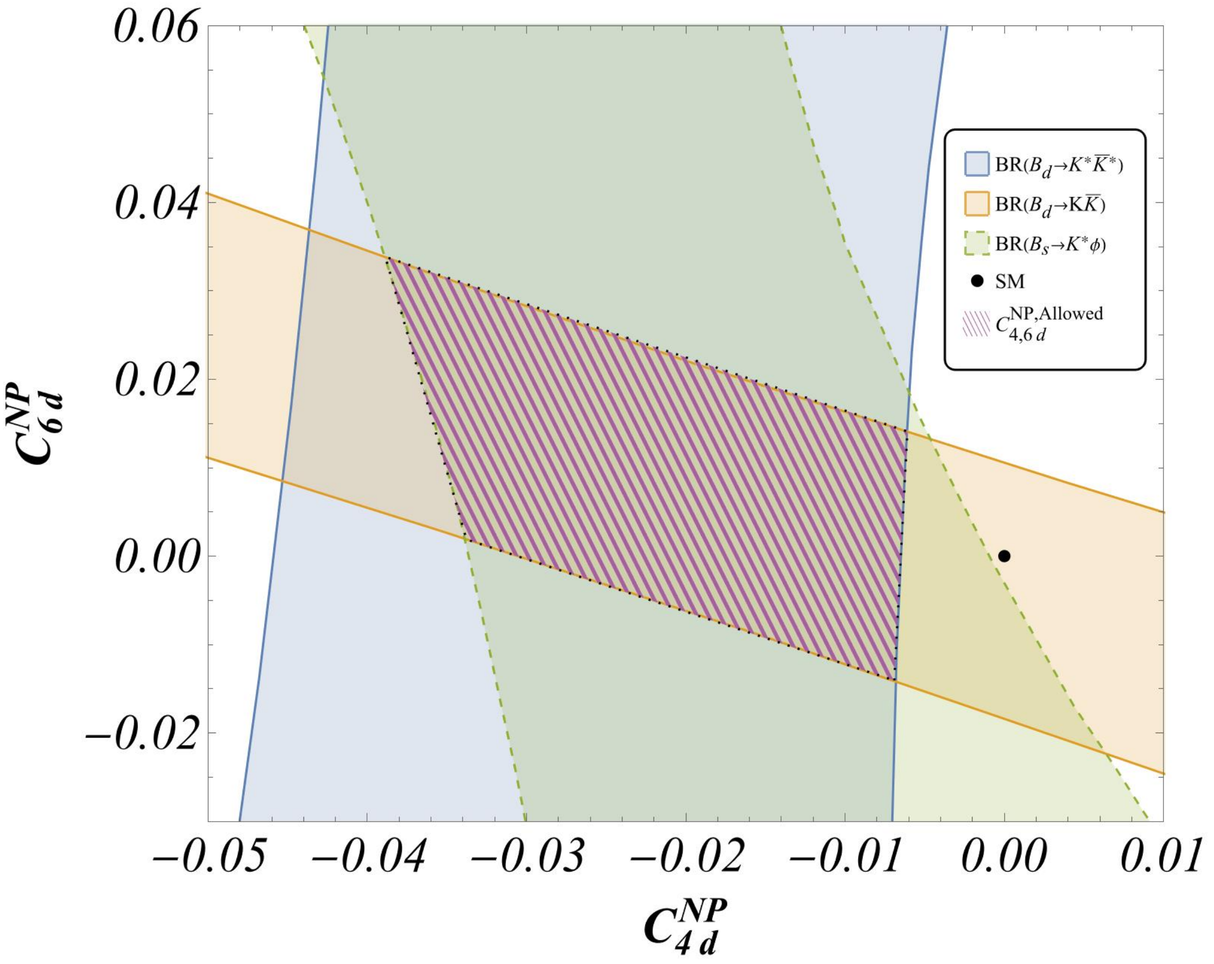

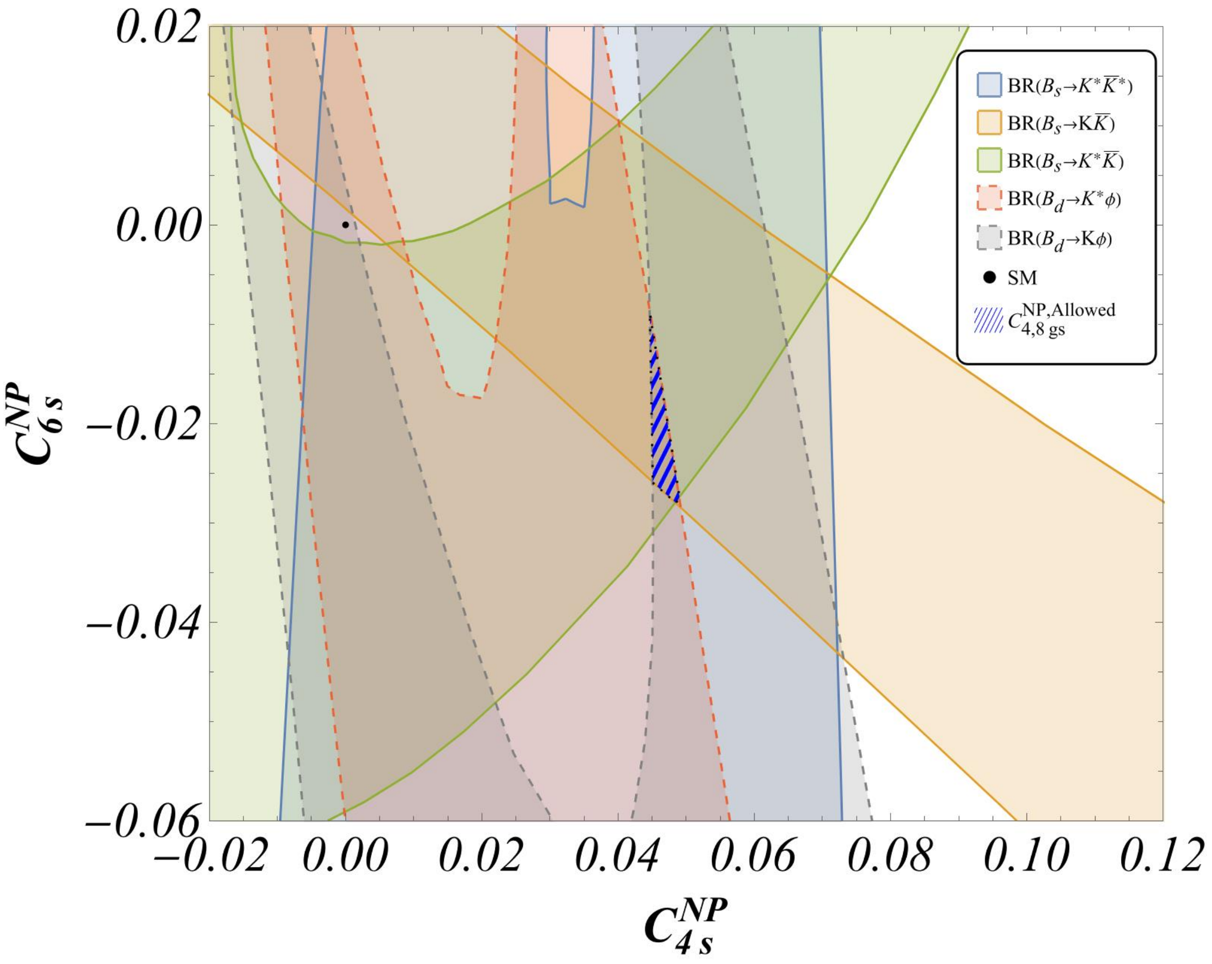

Two operator scenarios: $Q_6 - Q_{8g}$

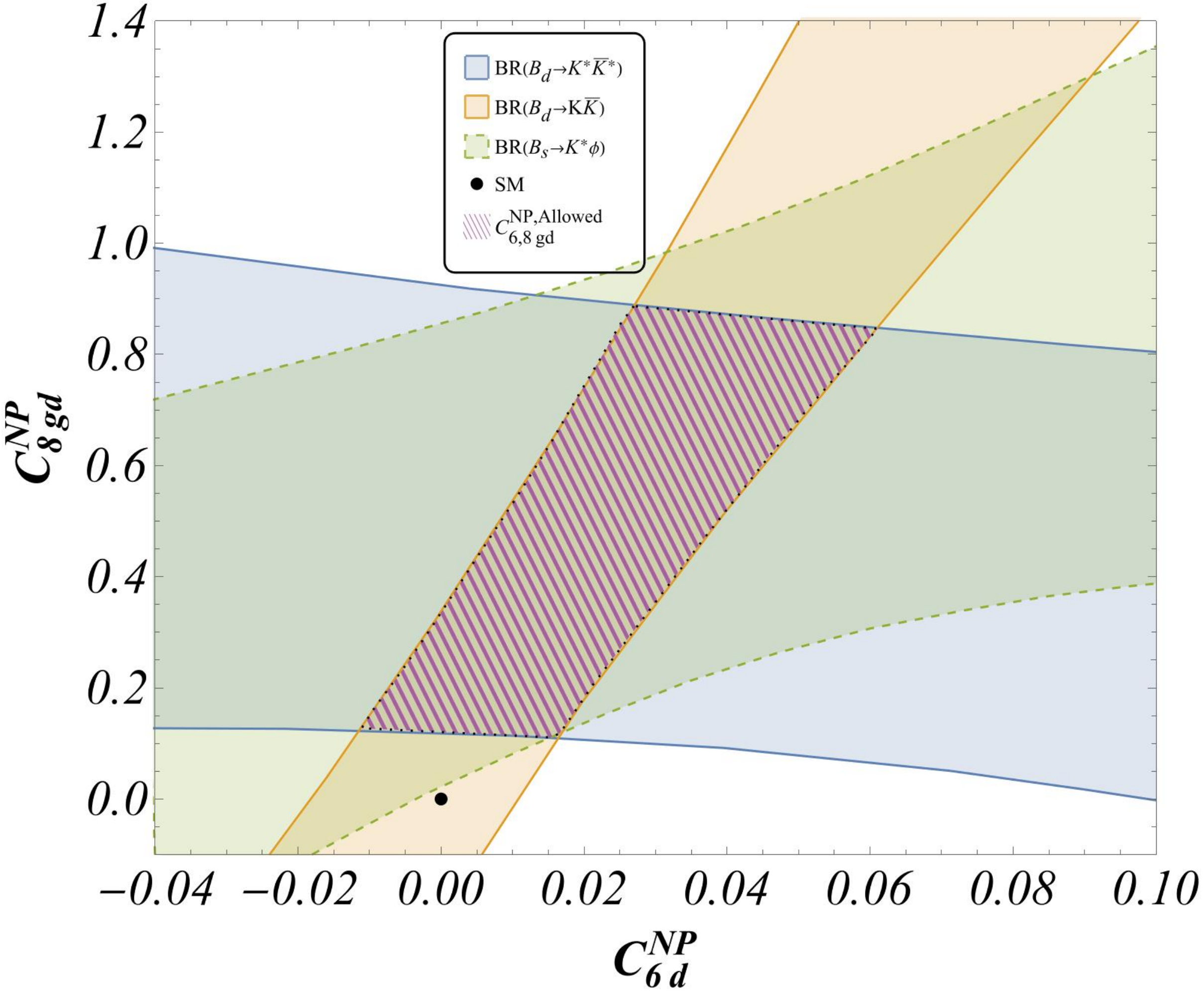

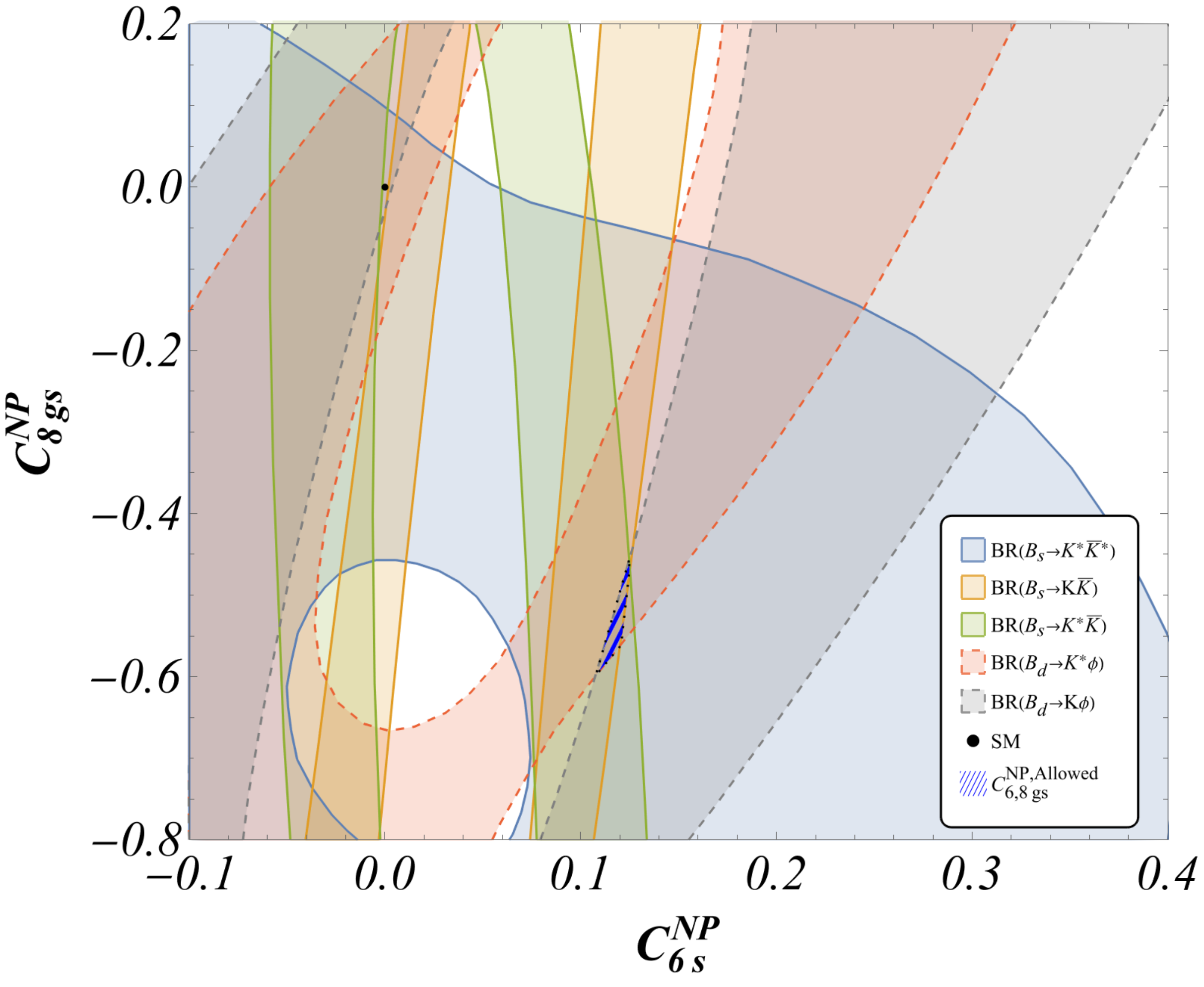

Two operator scenarios: $Q_4 - Q_{8g}$

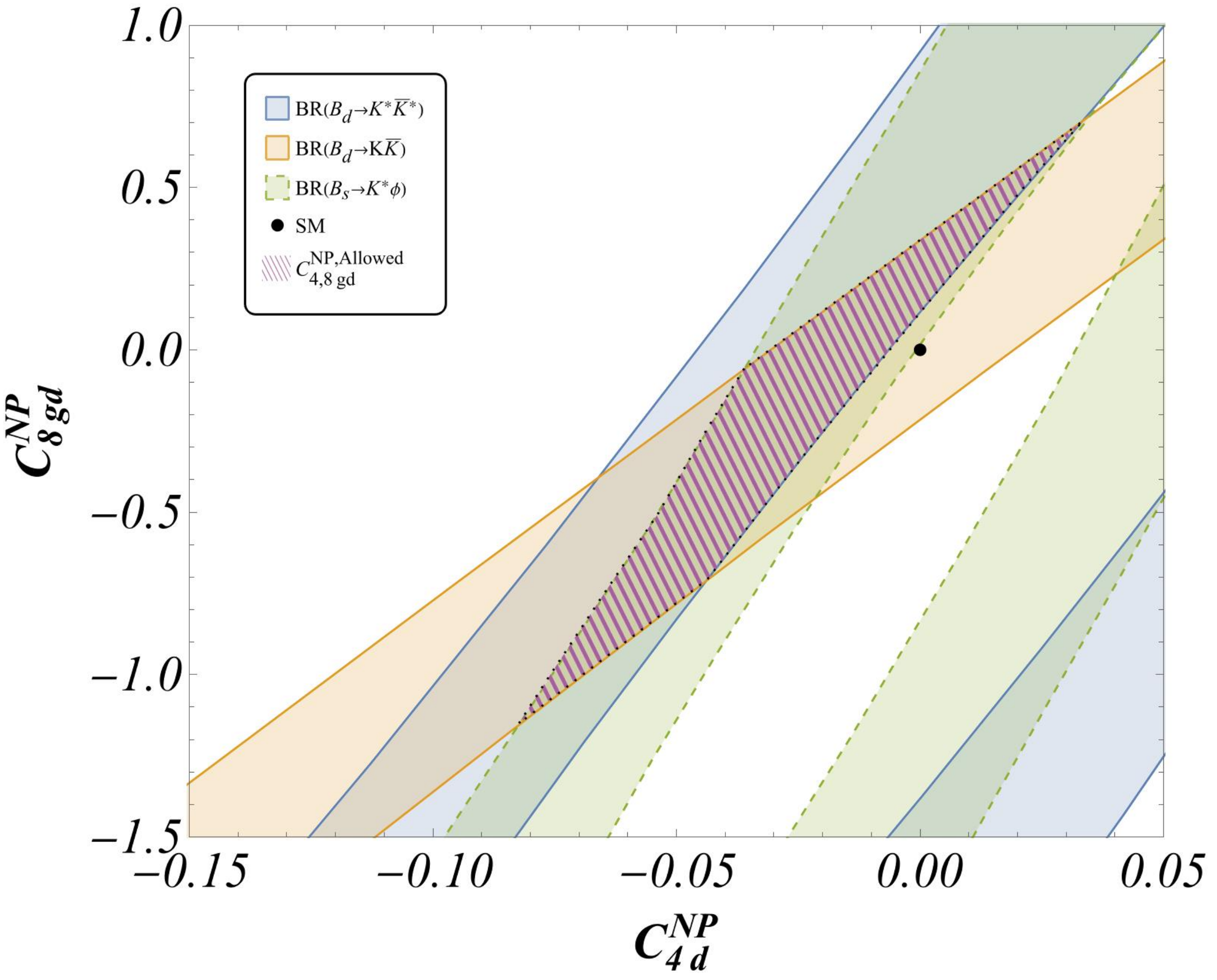

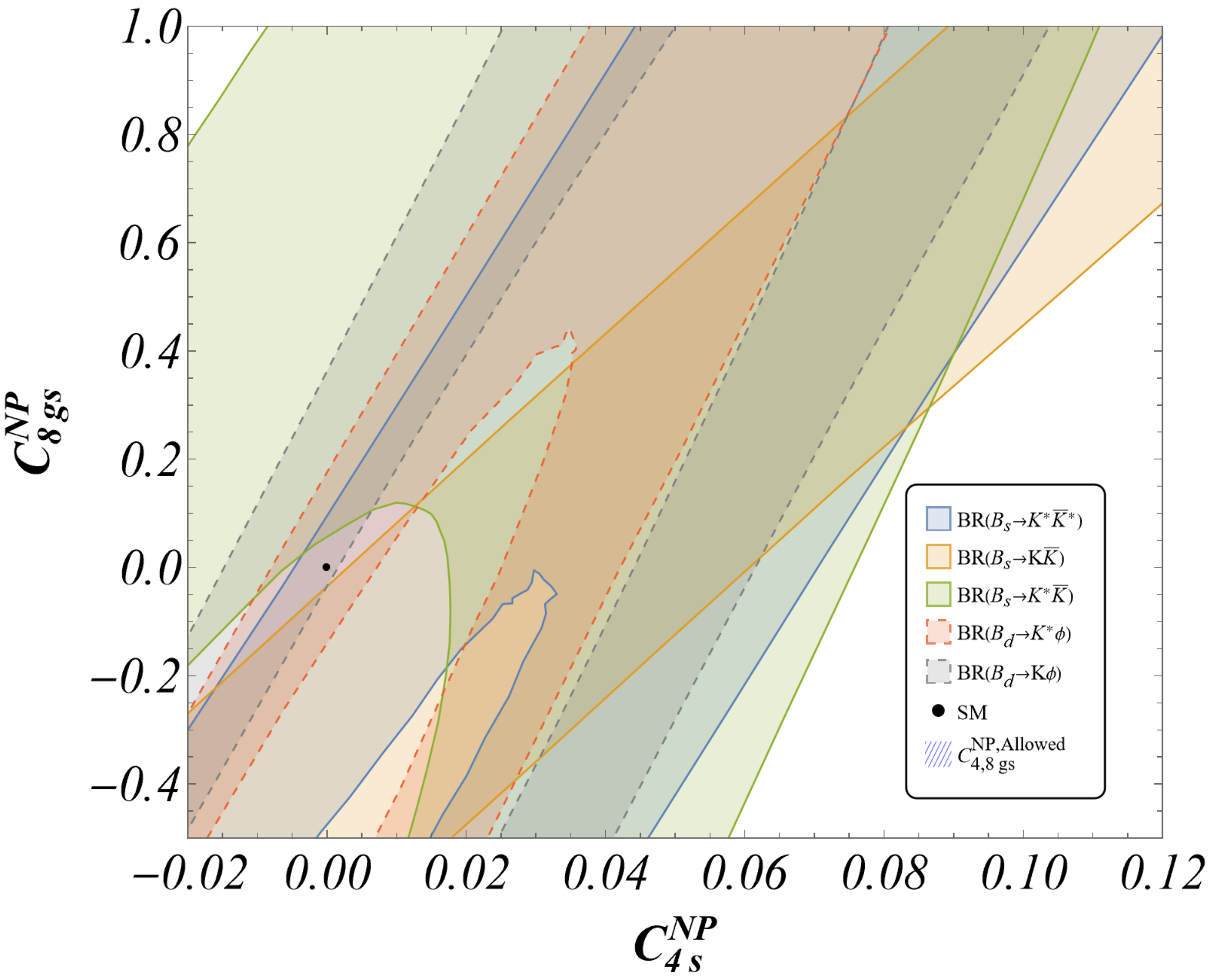

Theory vs experiment: Charged modes

Observable	SM (QCDF)	Experiment	Deviation
$10^6 BR(B^- \to K^{*-}\,\phi)$	$4.94^{+2.34}_{-1.91}$	$4.96^{+1.16}_{-1.08}$	*fully consistent*
$10^6 BR(B^- \to K^-\,\phi)$	$4.67^{+2.98}_{-1.63}$	$8.8^{+0.7}_{-0.6}$	1.5σ

Two operator scenarios: $Q_4 - Q_6$

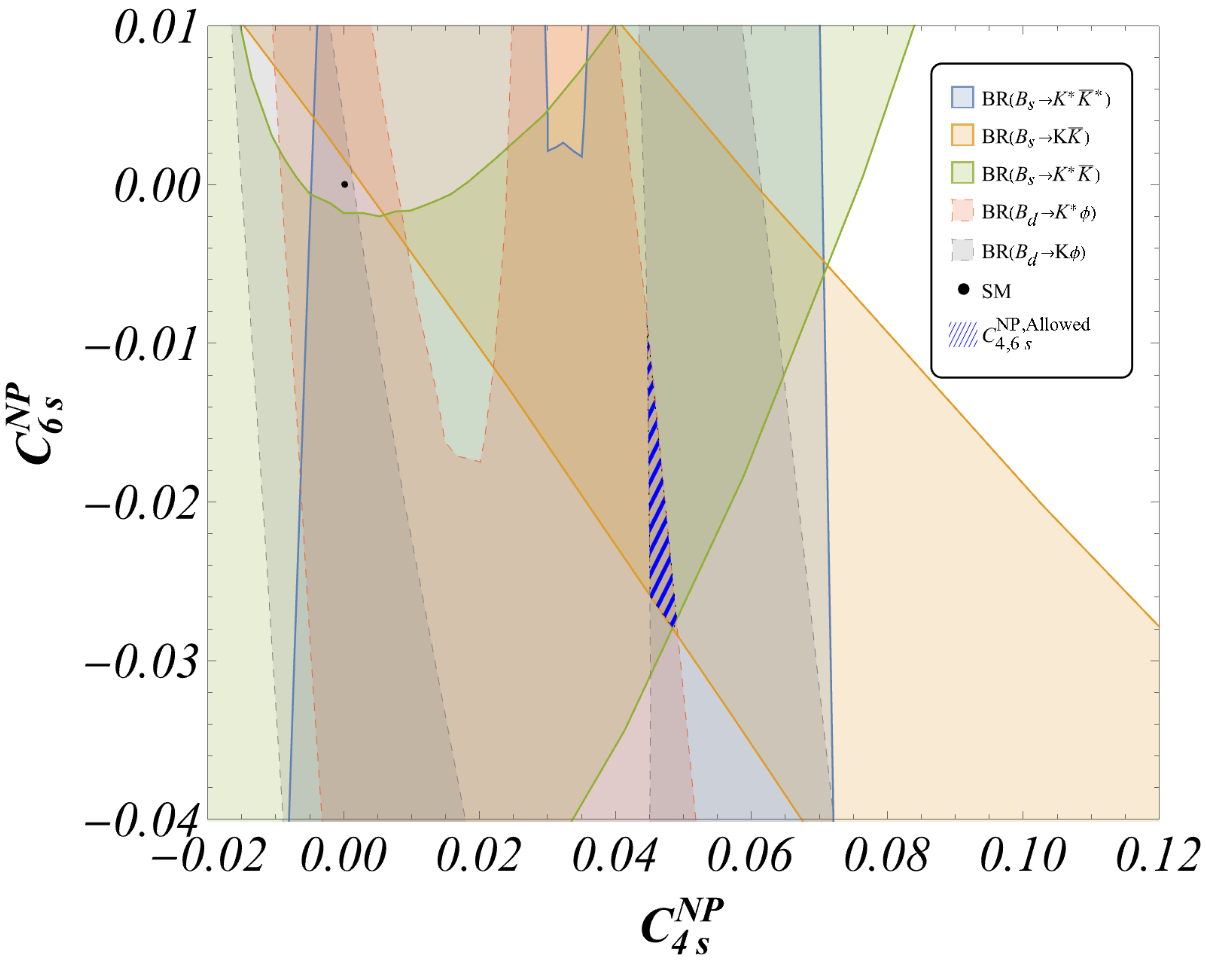

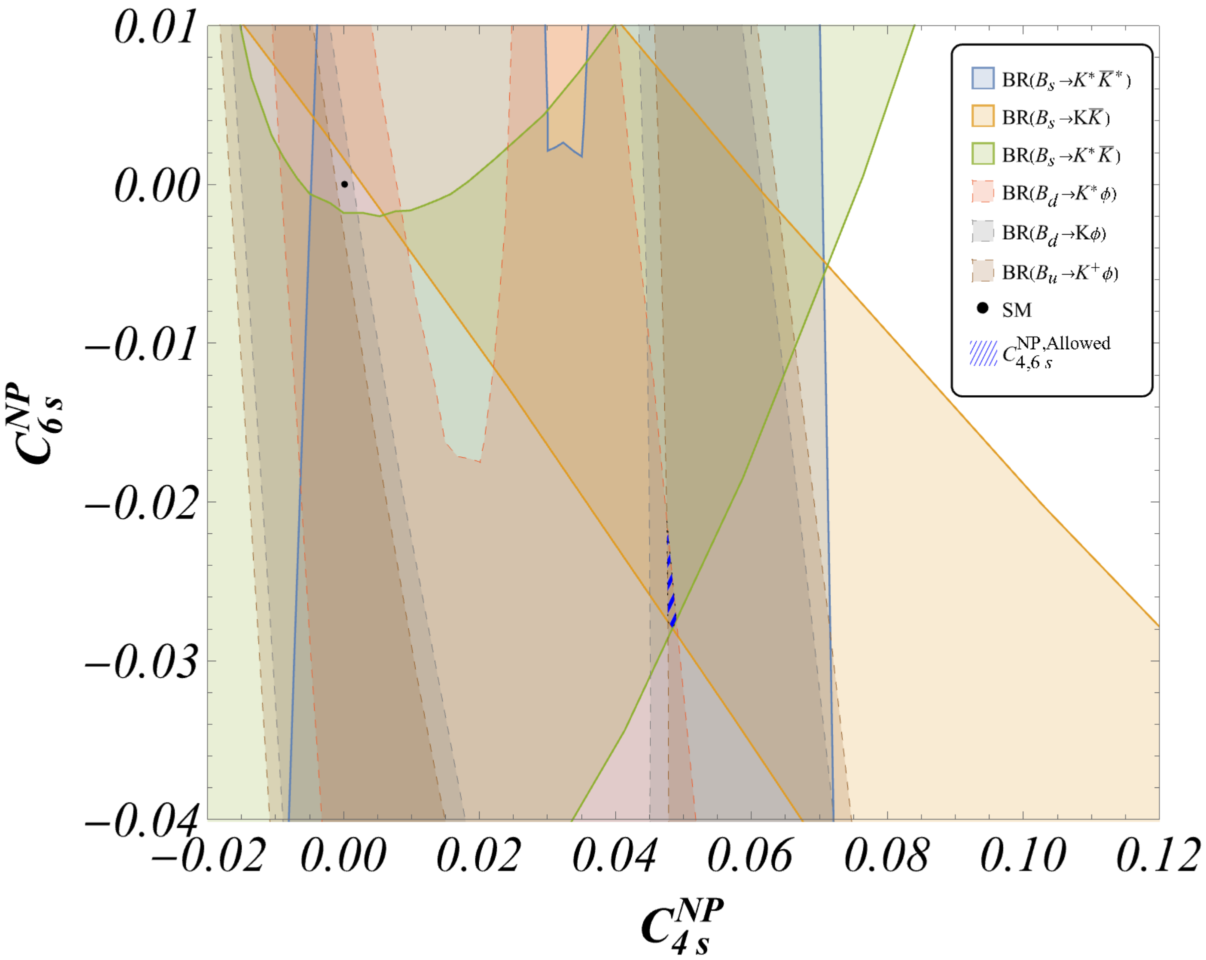

Two operator scenarios: $Q_4 - Q_6$

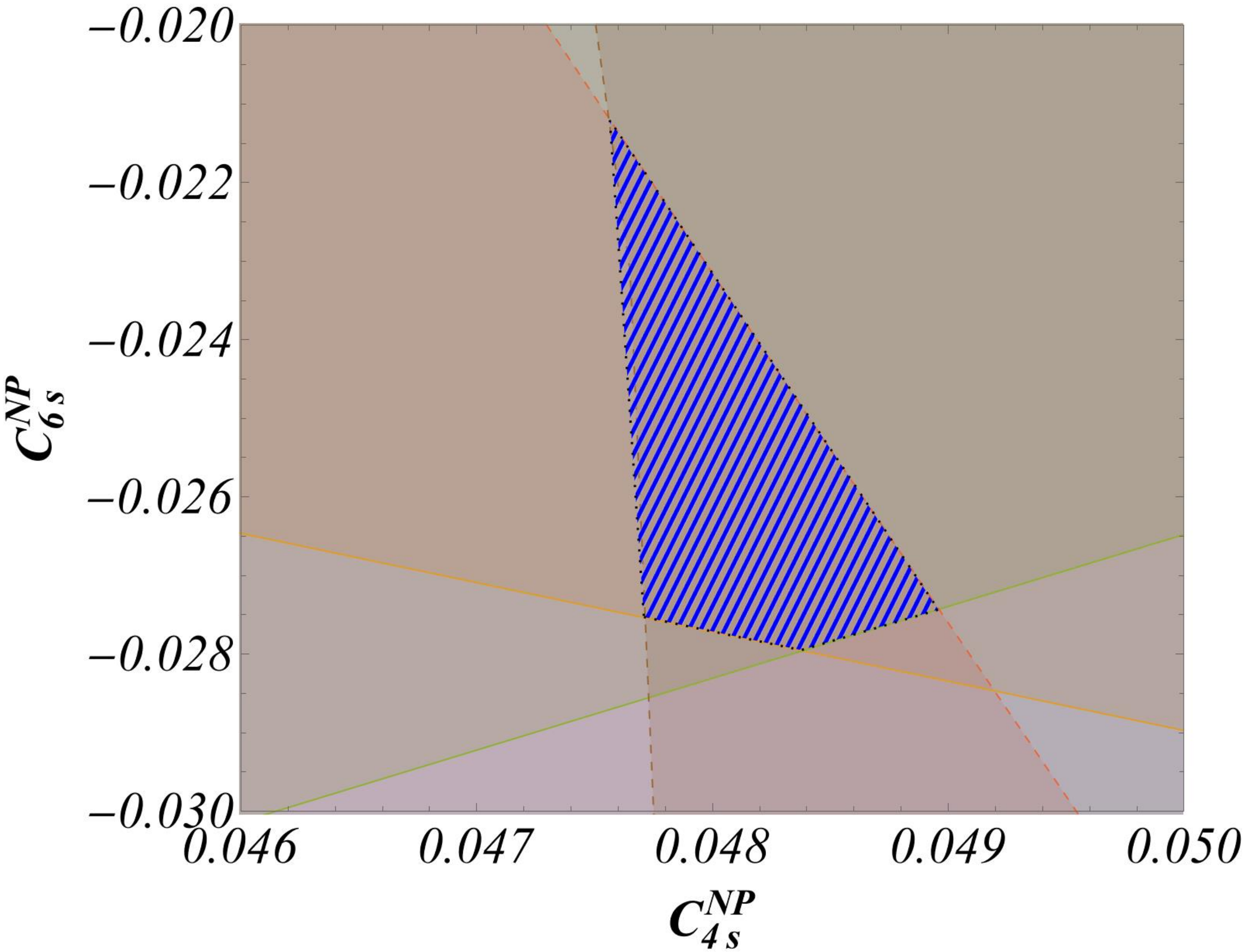

Zoomed in version showing the common region that explains all the seven b to s branching ratios for the $Q_4 - Q_6$ scenario.

Two operator scenarios: $Q_6 - Q_{8g}$

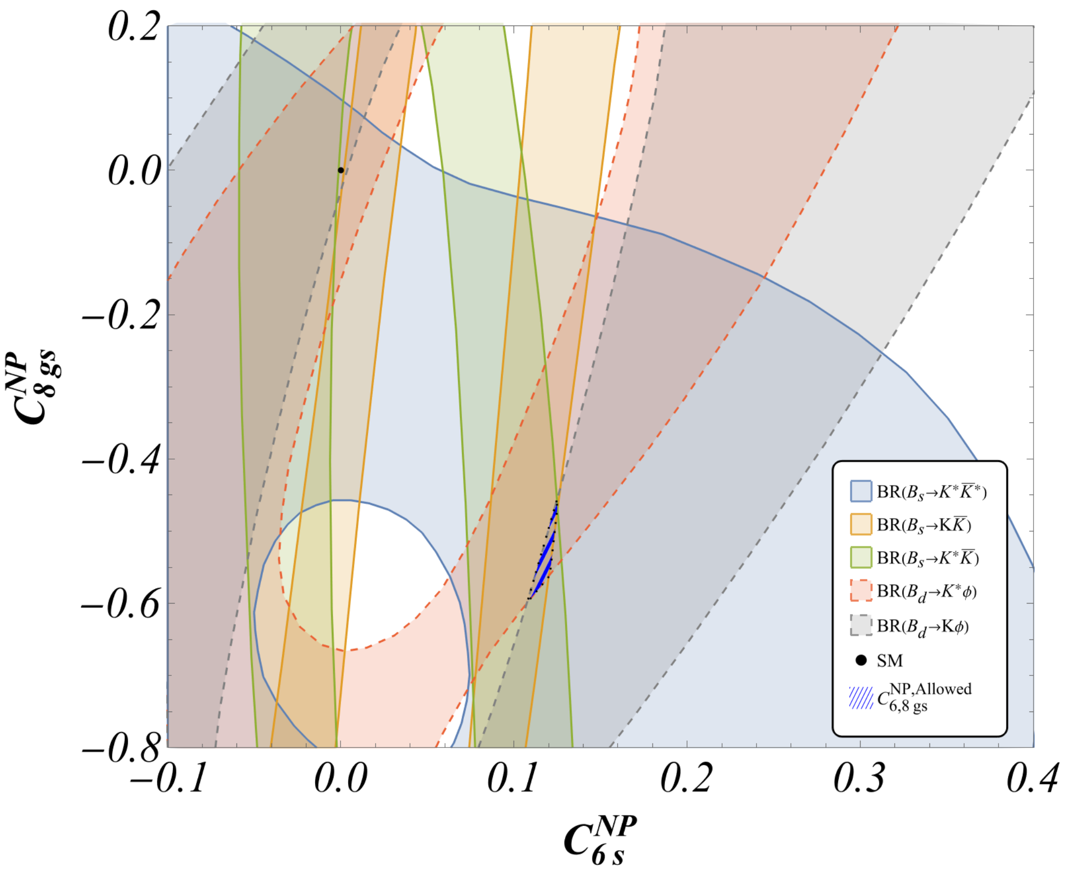

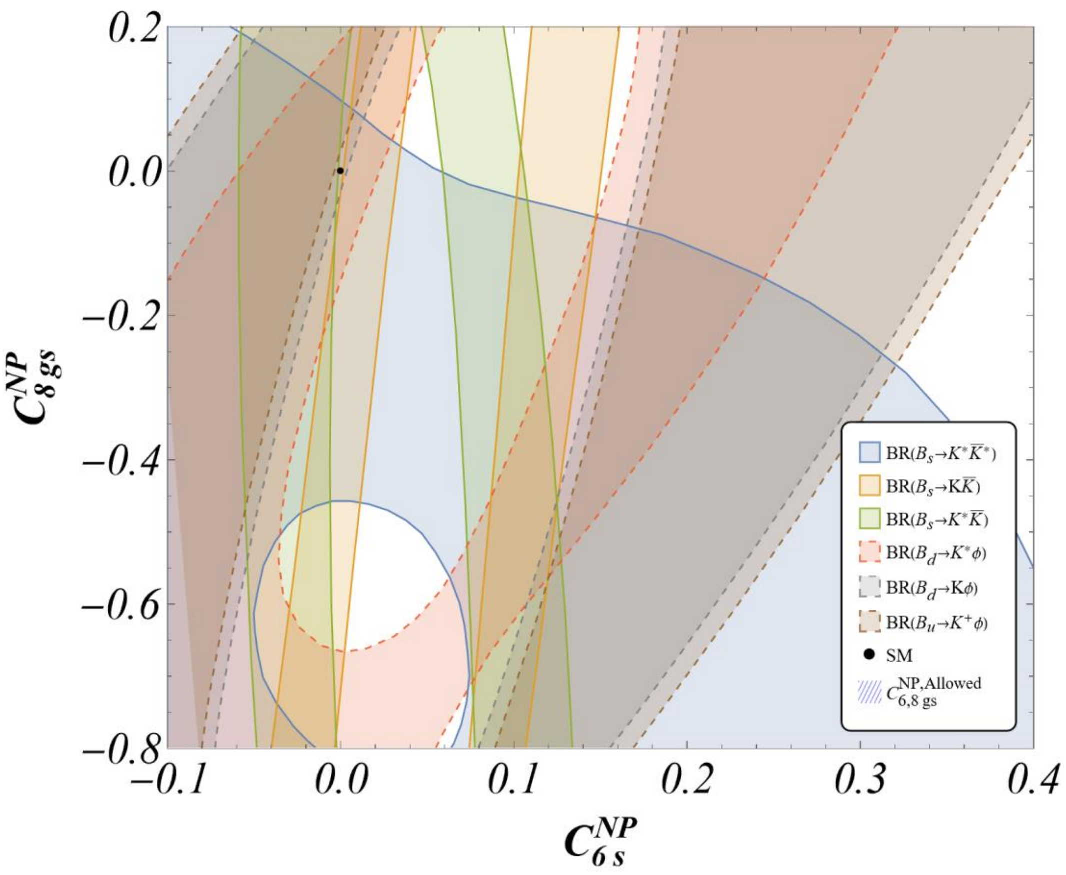

No common region that explains all the seven b to s branching ratios for the $Q_6 - Q_{8g}$ scenario.

Comparison: *SM*

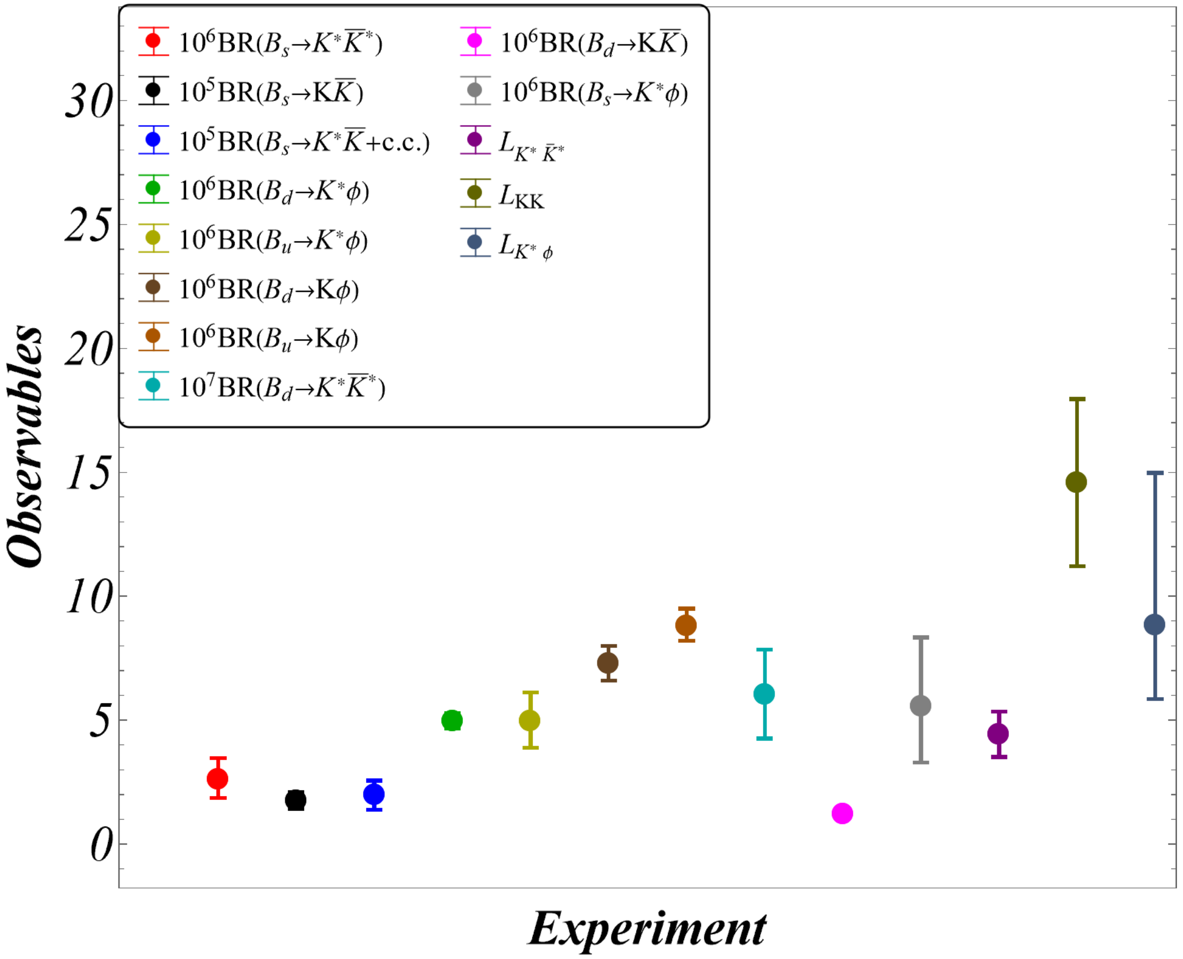

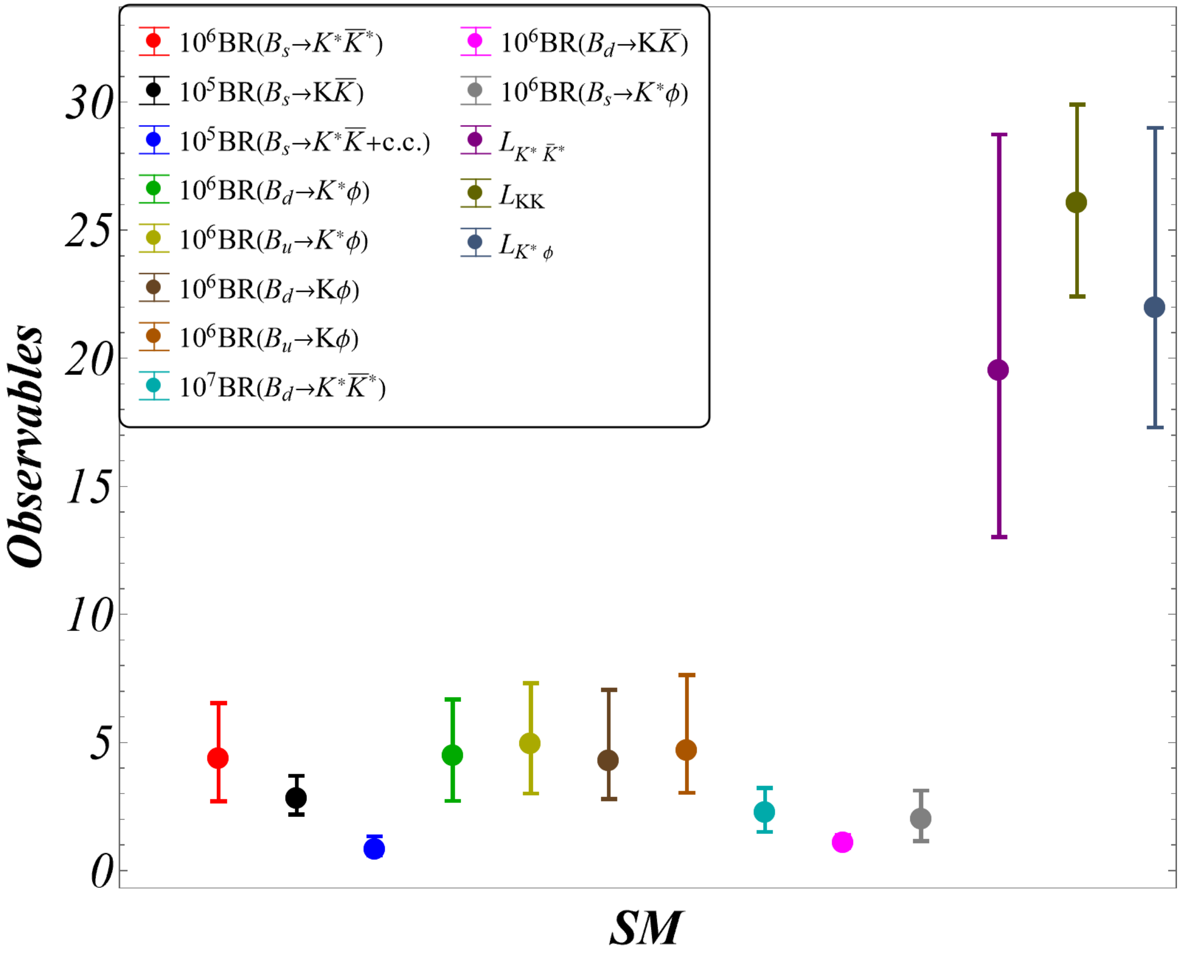

Comparison: $Q_4 - Q_6$

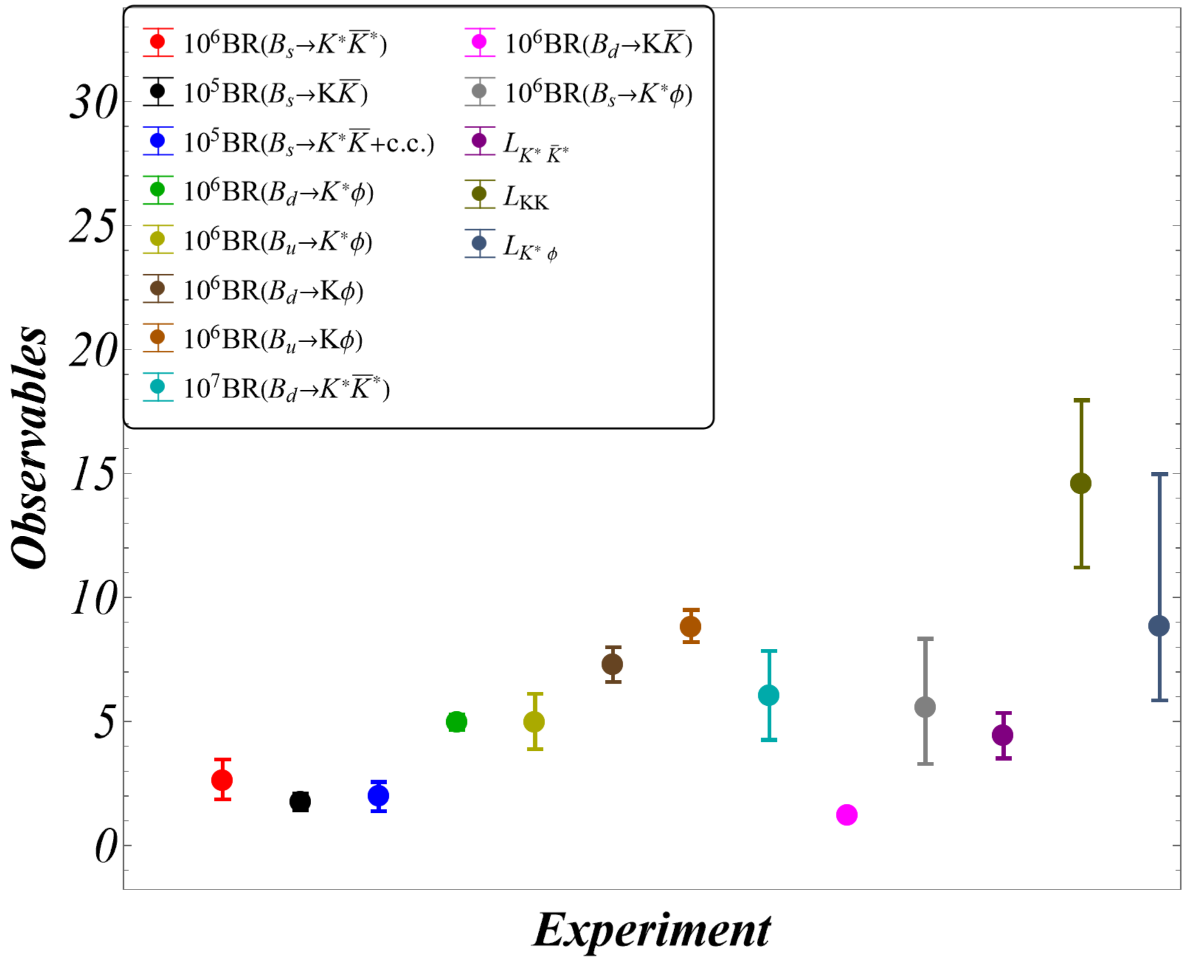

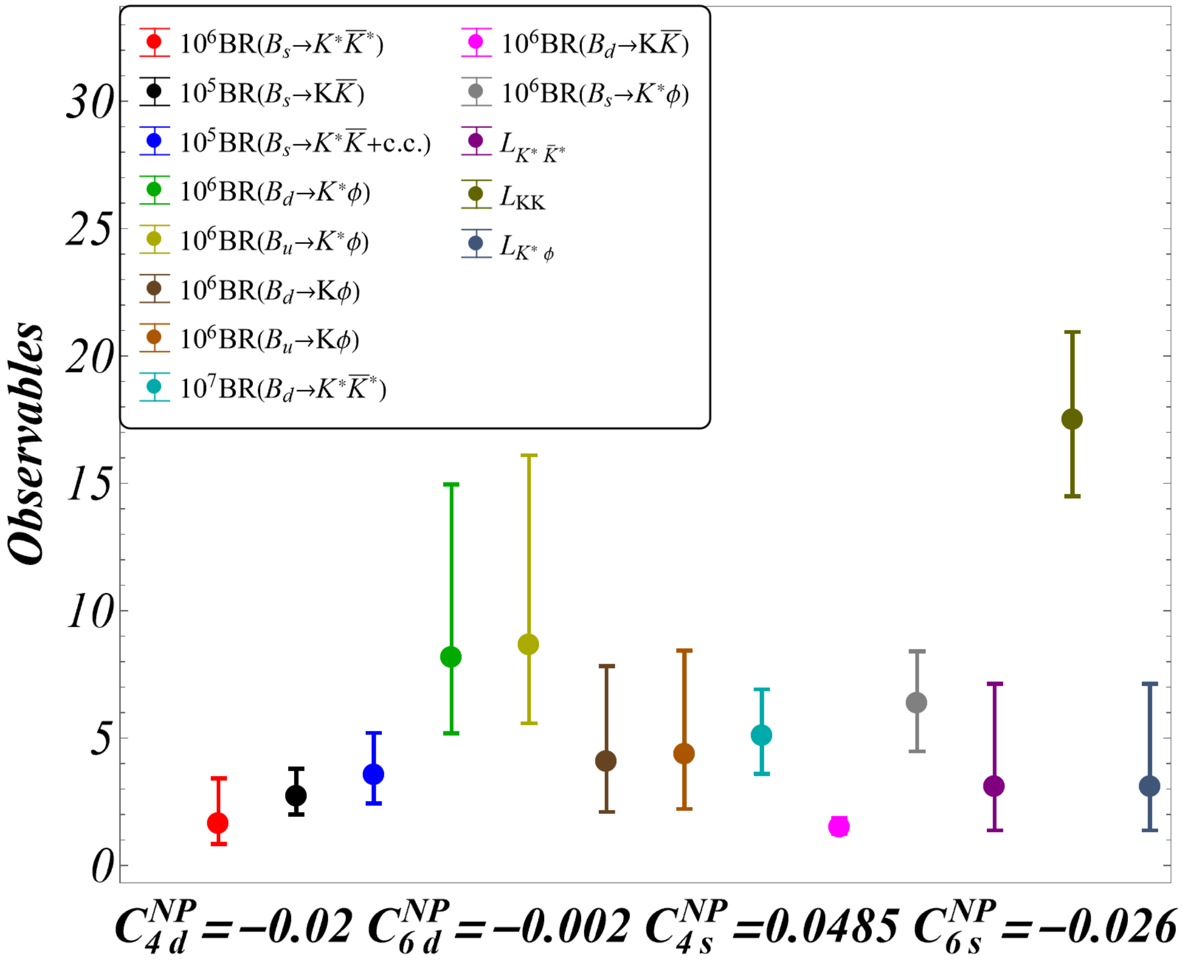

Conclusions

- Proposed optimized "L" observables which are ratios involving penguin dominated decay modes related by d to s interchange: only used while modelling the divergent annihilation and hard spectators.
- Dominant sources of uncertainties for theoretical SM estimates of the L's are form factors .
- All the VV, PP L's and branching ratios have overlaps assuming NP affects either $Q_{4d,s}$ or $Q_{8gd,s}$.
- However, the inclusion of the currently measured VP modes ruin this setup.
- The simplest NP scenario that results in common overlap among all the VV, PP and PV charged and neutral branching ratios as per the current data along with the three L's are 2 operator scenarios $Q_{4f} - Q_{6f}$.
- **$Q_{6d,s}$ is important!**
- Appeal to LHCb: Most recent measurements on $BR(\bar{B}_d(B^-) \to \bar{K}^0(K^-)\phi)$ more than a decade old. PDG average involves measurements by CDF, Babar, CLEO, Belle with rather different central values. No LHCb measurement. 1.5σ deviation between these measurements surprising because they are related by isospin. Maybe updated measurement can change this scenario. In particular, **these two measurements being consistent within 1σ with the current measurement for $BR(\bar{B}_d \to \bar{K}^0\phi)$ will make $Q_{6f} - Q_{8gf}$ a viable scenario.**

Future directions and discussions

- Correlated form factors (LCSR, Lattice)?
- Correlated measurement of Branching fractions. LHCb is already working on these modes: Anomalies 2024 (Ben & Davide).
- New ways of tackling annihilations: Fits. Breaking of universality. Analysis ongoing. Beyond Beneke etal: Symmetries and symmetry breakings. CP asymmetry measurements.
- $L_{K^*\phi}^{exp}$ has asymmetric errors. However, a correlated measurement in the future, as well as an increase in the precision of $f_L(\bar{B}_s \to K^{*0}\phi)$ and $BR(\bar{B}_s \to K^{*0}\phi)$ might help decrease the asymmetry. Measurement on $b \to d$ $BR(\bar{B}_s \to K^0\phi)$ and $BR(\bar{B}_d \to K^{*0}\bar{K}^0 + c.c.)$. Will permit construction of L's for mixed modes.
- First exploratory works. Working on rigorous statistical analysis taking asymmetric distributions into account. Possibility of three operator scenarios, complex Wilson coefficients etc.: Stay tuned!

THANK YOU!

Backup

$L_{K^*K^*}$

- $$L_{K^*K^*} = \kappa \left|\frac{P_s}{P_d}\right|^2 \left[\frac{1+|\alpha^s|^2\left|\frac{\Delta_s}{P_s}\right|^2 + 2Re\left(\frac{\Delta_s}{P_s}\right)Re(\alpha_s)}{1+|\alpha^d|^2\left|\frac{\Delta_d}{P_d}\right|^2 + 2Re\left(\frac{\Delta_d}{P_d}\right)Re(\alpha_d)}\right]$$

CKM

1 ± 0.3 (Naive SU(3))
$0.91^{+0.20}_{-0.17}$ (Broken SU(3))
$0.92^{+0.20}_{-0.18}$ (QCD factorization)
Dominant contribution

1 ± 0.01

- **Exp: $\mathbf{4.43 \pm 0.92}$**

SM: 23^{+16}_{-12} (Naive SU(3))
$19.2^{+9.3}_{-6.5}$ (Broken SU(3))
$\mathbf{19.53^{+9.14}_{-6.64}}$ (QCD factorization)

- **Tension: $\mathbf{2.6\sigma}$**

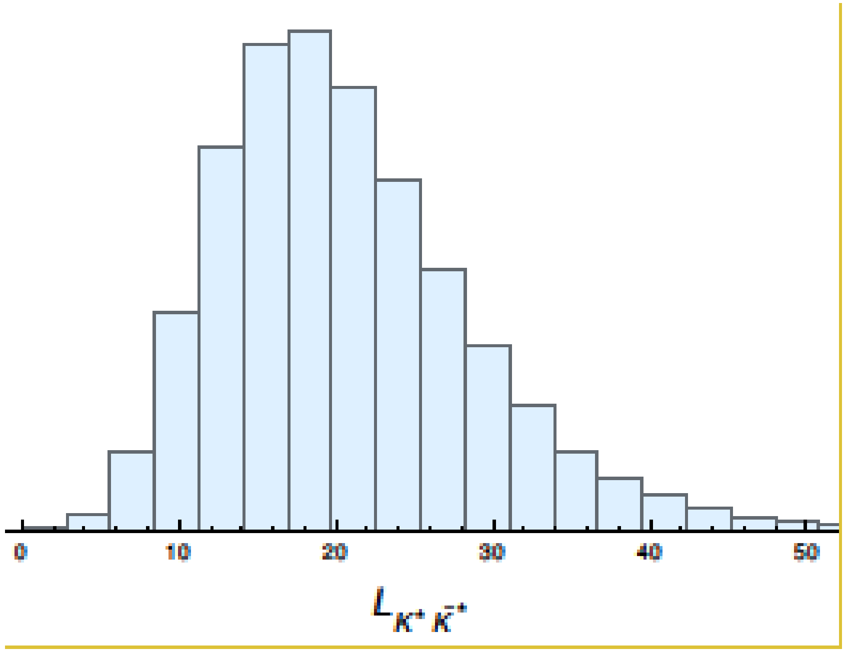

- Note: Dominant uncertainties from form factors and NOT divergences. (Somewhat) reduced model dependence.

$L_{K^*K^*}$: Error Budget

	Relative Error		
Input	$L_{K^*\bar{K}^*}$	$\|P_s\|^2$	$\|P_d\|^2$
f_{K^*}	$(-0.1\%, +0.1\%)$	$(-6.8\%, +7.1\%)$	$(-6.8\%, +7\%)$
$A_0^{B_d}$	$(-22\%, +32\%)$	—	$(-24\%, +28\%)$
$A_0^{B_s}$	$(-28\%, +33\%)$	$(-28\%, +33\%)$	—
λ_{B_d}	$(-0.6\%, +0.2\%)$	$(-4.6\%, +2.1\%)$	$(-4.1\%, +1.9\%)$
$\alpha_2^{K^*}$	$(-0.1\%, +0.1\%)$	$(-3.6\%, +3.7\%)$	$(-3.6\%, +3.6\%)$
X_H	$(-0.2\%, +0.2\%)$	$(-1.8\%, +1.8\%)$	$(-1.6\%, +1.6\%)$
X_A	$(-4.3\%, +4.4\%)$	$(-17\%, +19\%)$	$(-13\%, +14\%)$
κ	$(-1.4\%, +2.2\%)$	—	—
Others	$(-1.3\%, +1.1\%)$	$(-2.7\%, +2.5\%)$	$(-1.6\%, +1.6\%)$

Table 2. Error budget of $L_{K^*\bar{K}^*}$ and $|P_{d,s}|^2$. The relative error of each theoretical input is obtained by varying them individually. The main sources of uncertainty are the form factors, followed by weak annihilation at a significantly smaller level.

$B_{d,s}$ Distribution Amplitudes (at $\mu = 1$ GeV) [34, 35]		
λ_{B_d} [GeV]	$\lambda_{B_s}/\lambda_{B_d}$	σ_B
0.383 ± 0.153	1.19 ± 0.14	1.4 ± 0.4

K^* Distribution Amplitudes (at $\mu = 2$ GeV) [36]			
$\alpha_1^{K^*}$	$\alpha_{1,\perp}^{K^*}$	$\alpha_2^{K^*}$	$\alpha_{2,\perp}^{K^*}$
0.02 ± 0.02	0.03 ± 0.03	0.08 ± 0.06	0.08 ± 0.06

ϕ Distribution Amplitudes (at $\mu = 2$ GeV) [36]			
α_1^{ϕ}	$\alpha_{1,\perp}^{\phi}$	α_2^{ϕ}	$\alpha_{2,\perp}^{\phi}$
0	0	0.13 ± 0.06	0.11 ± 0.05

Decay Constants for B mesons (at $\mu = 2$ GeV) [37] and K meson [28]		
f_{B_d}	f_{B_s}/f_{B_d}	f_K
0.190 ± 0.0013	1.209 ± 0.005	0.1557 ± 0.0003

Decay Constants for K^*, ϕ, ρ, ω (at $\mu = 2$ GeV) [26, 38]					
f_{K^*}	$f_{K^*}^{\perp}/f_{K^*}$	f_ϕ	$f_\phi^{\perp}/f_\phi$	f_ρ	f_ω
0.204 ± 0.007	0.712 ± 0.012	0.233 ± 0.004	0.750 ± 0.008	0.213 ± 0.005	0.197 ± 0.008

$B_{d,s} \to K^*, \phi$ form factors [26] and B-meson lifetimes (ps) [39]				
$A_0^{B_s \to K^*}(q^2 = m_\phi^2)$	$A_0^{B_d \to K^*}(q^2 = m_\phi^2)$	$A_0^{B_s \to \phi}(q^2 = m_{K^*}^2)$	τ_{B_d}	τ_{B_s}
0.380 ± 0.024	0.393 ± 0.039	0.438 ± 0.024	1.519 ± 0.004	1.520 ± 0.005

Mass and decay widths for ρ, ω (GeV) [28]			
m_ρ	Γ_ρ	m_ω	Γ_ω
0.7745	0.1484	0.7827	0.0087

$B_d \to K$ [25], $B_s \to K$ [40] and $B_s \to \phi$ form factors		
$f_0^{B_s}(q^2 = m_\phi^2)$	$f_0^{B_d}(q^2 = m_\phi^2)$	$A_0^{B_s \to \phi}(q^2 = m_K^2)$
0.336 ± 0.023	0.340 ± 0.011	0.426 ± 0.024

Wolfenstein parameters [41]			
A	λ	$\bar{\rho}$	$\bar{\eta}$
$0.8132^{+0.0119}_{-0.0060}$	$0.22500^{+0.00024}_{-0.00022}$	$0.1566^{+0.0085}_{-0.0048}$	$0.3475^{+0.0118}_{-0.0054}$

QCD scale and masses [GeV] [28]							
$\bar{m}_b(\bar{m}_b)$	m_b/m_c	m_{B_d}	m_{B_s}	m_{K^*}	m_ϕ	m_K	$\Lambda_{\rm QCD}$
4.18	4.577 ± 0.008	5.27966	5.36692	0.89555	1.01946	0.497611	0.225

SM Wilson Coefficients (at $\mu = 4.18$ GeV)					
$\mathcal{C}_1$	$\mathcal{C}_2$	$\mathcal{C}_3$	$\mathcal{C}_4$	$\mathcal{C}_5$	$\mathcal{C}_6$
1.082	-0.191	0.014	-0.036	0.009	-0.042
$\mathcal{C}_7/\alpha_{em}$	$\mathcal{C}_8/\alpha_{em}$	$\mathcal{C}_9/\alpha_{em}$	$\mathcal{C}_{10}/\alpha_{em}$	$\mathcal{C}_{7\gamma}^{\rm eff}$	$\mathcal{C}_{8g}^{\rm eff}$
-0.011	0.060	-1.254	0.224	-0.318	-0.151

	MLR	CDF
$L_{K^*\bar{K}^*}$	$17.2^{+8.3}_{-5.9}$	$19.5^{+9.1}_{-6.7}$
$L_{K\bar{K}}$	$25.5^{+4.0}_{-3.3}$	$26.0^{+3.9}_{-3.6}$
$\hat{L}_{K^*}$	$20.5^{+6.8}_{-6.2}$	$21.3^{+7.2}_{-6.3}$
$\hat{L}_{K}$	$25.3^{+3.7}_{-4.5}$	$25.0^{+4.2}_{-4.1}$
L_{K^*}	$16.6^{+6.9}_{-6.0}$	$17.4^{+6.6}_{-5.8}$
L_{K}	$28.8^{+5.2}_{-4.6}$	$29.2^{+5.5}_{-5.3}$
$L_{\rm total}$	$23.5^{+3.8}_{-4.0}$	$23.5^{+4.0}_{-3.8}$
R_d	$0.67^{+0.23}_{-0.24}$	$0.70^{+0.30}_{-0.22}$
$\mathcal{B}(B_d \to K^{*0}\bar{K}^{*0}) \times 10^6$	$0.22^{+0.08}_{-0.08}$	$0.23^{+0.10}_{-0.08}$
$\mathcal{B}(B_s \to K^{*0}\bar{K}^{*0}) \times 10^6$	$3.95^{+1.88}_{-1.54}$	$4.36^{+2.23}_{-1.65}$
$\mathcal{B}(B_d \to K^{0}\bar{K}^{0}) \times 10^6$	$1.01^{+0.24}_{-0.16}$	$1.09^{+0.29}_{-0.20}$
$\mathcal{B}(B_s \to K^{0}\bar{K}^{0}) \times 10^6$	$25.6^{+7.5}_{-5.2}$	$28.0^{+8.9}_{-6.2}$

α_i coefficients $\to a_i$ [BBNS]

$$a_i^p(M_1M_2) = \left(C_i + \frac{C_{i\pm1}}{N_c}\right) N_i(M_2) + \frac{C_{i\pm1}}{N_c}\frac{C_F\alpha_s}{4\pi}\left[V_i(M_2) + \frac{4\pi^2}{N_c} H_i(M_1M_2)\right] + P_i^p(M_2)\,,$$

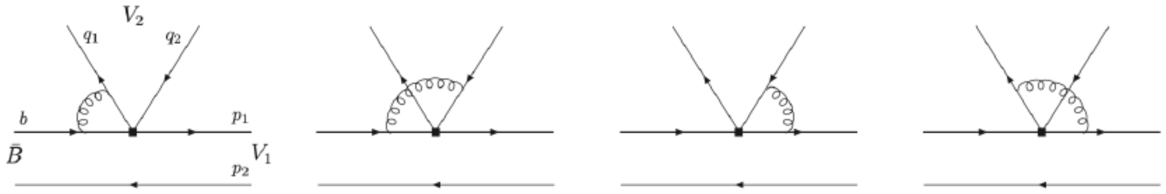

Figure 1: Vertex diagrams.

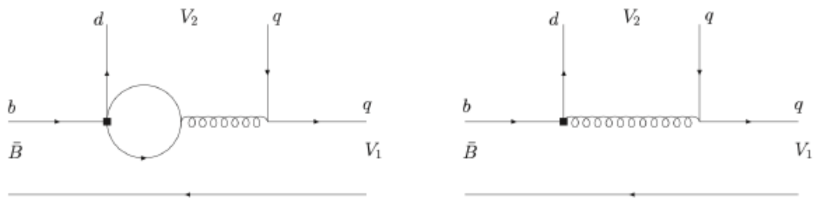

Figure 2: Penguin diagrams.

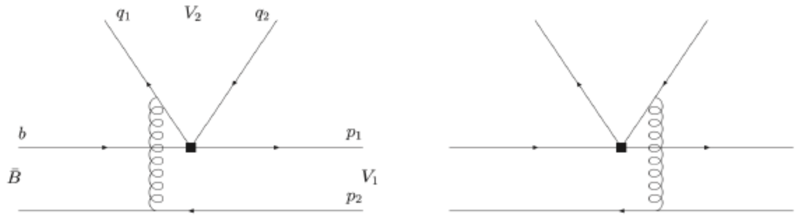

Figure 3: Hard spectator diagrams.

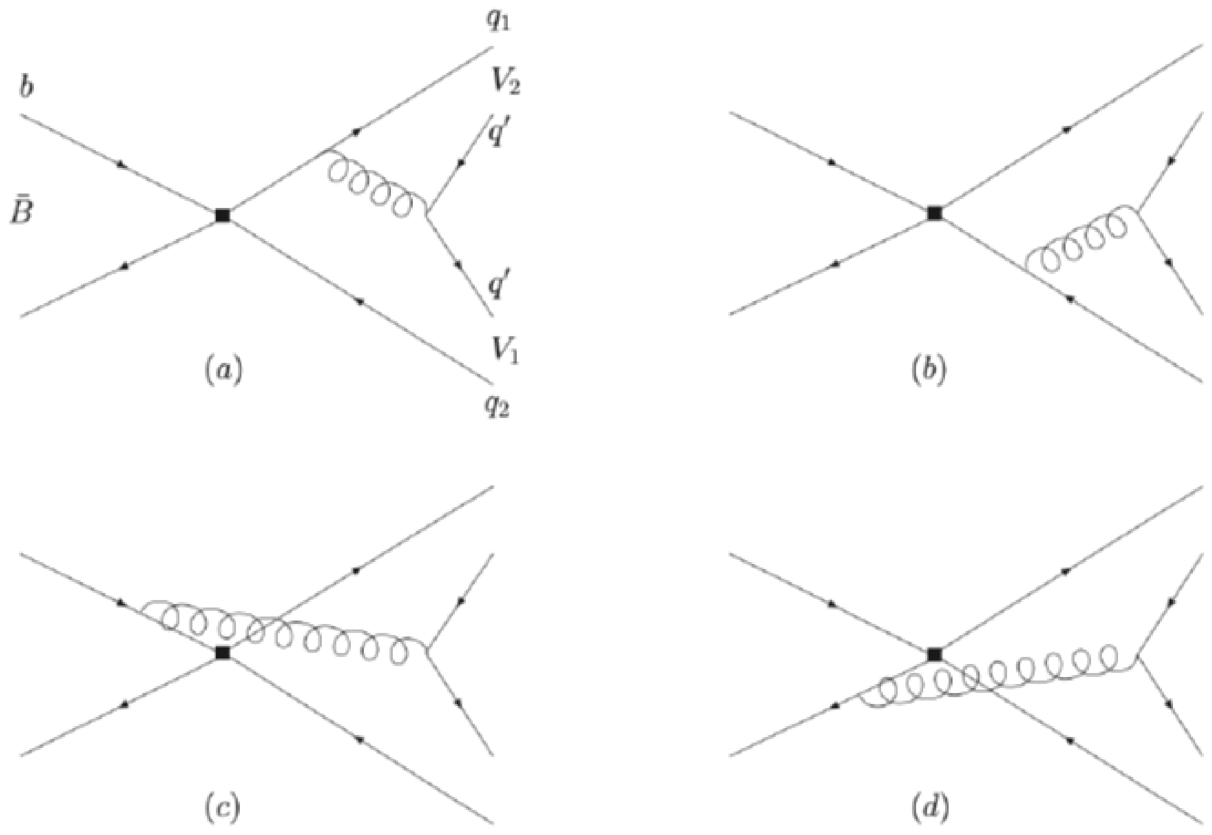

Figure 4: Annihilation diagrams.

Main caveat:

(Existence of some) **Power suppressed** but **IR divergent** spectator scattering and weak annihilation that affects amplitudes: